



# Meta-QTLs, ortho-MQTLs and candidate genes for nitrogen use efficiency and root system architecture in bread wheat (*Triticum aestivum* L.)

Dinesh Kumar Saini<sup>1</sup> · Yuvraj Chopra<sup>2,5</sup> · Neeraj Pal<sup>3</sup> · Amneek Chahal<sup>2</sup> ·  
Puja Srivastava<sup>1</sup> · Pushpendra Kumar Gupta<sup>4</sup>

Received: 23 July 2021 / Revised: 26 September 2021 / Accepted: 27 September 2021 / Published online: 4 October 2021  
© Prof. H.S. Srivastava Foundation for Science and Society 2021

**Abstract** In wheat, meta-QTLs (MQTLs), ortho-MQTLs, and candidate genes (CGs) were identified for nitrogen use efficiency and root system architecture. For this purpose, 1788 QTLs were available from 24 studies published during 2006–2020. Of these, 1098 QTLs were projected onto the consensus map resulting in 118 MQTLs. The average confidence interval (CI) of MQTLs was reduced up to 8.56 folds in comparison to the average CI of QTLs. Of the 118 MQTLs, 112 were anchored to the physical map of the wheat reference genome. The physical interval of MQTLs ranged from 0.02 to 666.18 Mb with a mean of 94.36 Mb. Eighty-eight of these 112 MQTLs were verified by marker-trait associations (MTAs) identified in published genome-wide association studies (GWAS); the MQTLs that were verified using GWAS also included 9 most robust MQTLs, which are particularly useful for breeders; we call them ‘Breeder’s QTLs’. Some selected wheat MQTLs were further utilized for the identification of ortho-MQTLs for wheat and maize; 9 such ortho-MQTLs were available. As many as 1991 candidate genes (CGs) were also

detected, which included 930 CGs with an expression level of > 2 transcripts per million in relevant organs/tissues. Among the CGs, 97 CGs with functions previously reported as important for the traits under study were selected. Based on homology analysis and expression patterns, 49 orthologues of 35 rice genes were also identified in MQTL regions. The results of the present study may prove useful for the improvement of selection strategy for yield potential, stability, and performance under N-limiting conditions.

**Keywords** Meta-QTL analysis · Breeder’s QTLs · Candidate genes · Orthologues

## Introduction

Nitrogen (N) is a major limiting factor for plant growth and development (Raun and Johnson 1999) so that during the four decades of the green revolution, a seven-fold rise in the use of nitrogen fertilizer was needed to achieve the doubling of agricultural food production worldwide (Hirel et al. 2007). A side-effect of this excess use of N has also been witnessed in the form of a negative impact on the ecosystem (Li et al. 2015). In order to limit the excess use of N without any adverse effect on yield, the use of cultivars with improved efficiency for N uptake and utilization has been recommended, particularly under low N input management (Good and Beatty 2011). In wheat, the availability of genetic variation in the germplasm suggests that the development of cultivars with high nitrogen use efficiency (NUE) is possible and can be achieved through breeding (Balyan et al. 2016). However, due to the complex genetic architecture of this trait and strong genotype-environment interactions (G × E) involved, efforts for

✉ Pushpendra Kumar Gupta  
pkgupta36@gmail.com

<sup>1</sup> Department of Plant Breeding and Genetics, Punjab Agricultural University, Ludhiana 141004, India  
<sup>2</sup> College of Agriculture, Punjab Agricultural University, Ludhiana 141004, India  
<sup>3</sup> Department of Molecular Biology and Genetic Engineering, G. B. Pant, University of Agriculture and Technology, Pantnagar, Uttarakhand 263145, India  
<sup>4</sup> Department of Genetics and Plant Breeding, Ch. Charan Singh University, Meerut 250004, India  
<sup>5</sup> Present Address: Department of Agronomy and Horticulture, University of Nebraska-Lincoln, Lincoln, NE 68583, USA

breeding wheat cultivars for high NUE met with only limited success.

NUE is commonly defined as grain yield per unit of N supplied (Moll et al. 1982); it largely depends on two major components: Nitrogen Uptake Efficiency (NUpE) and Nitrogen Utilization Efficiency (NUtE). NUpE is the quantity of N taken up by the plant per unit of N provided, whereas, NUtE is the grain yield per unit of N taken up by the plant. As a result, NUE is only the sum of NUpE and NUtE (Moll et al. 1982; Good et al. 2004). Other traits that are most relevant for measuring NUE in wheat include the following, besides others: (i) chlorophyll content, (ii) plant height, (iii) biomass, (iv) fresh and dry weight of plants, (v) N accumulation partitioning indices, (vi) leaf area index, (vii) grain N, (viii) grain protein content, (ix) enzymatic activities in different plant parts/tissues, (x) agronomic traits such as grain number, grain weight, grain filling duration, days to heading/flowering/maturity, tiller number, and spike related traits (Greef 1994; Cirilo et al. 2009; Sun et al. 2013; Balyan et al. 2016; Brasier et al. 2020). Root system architecture (RSA) is also critical while breeding for high NUpE (Lopez-Bucio et al. 2003; Garnett et al. 2009). A desirable root RSA for improved NUpE, particularly under low-N soils, includes increase in root dry weight, root length, root density, root number, root diameter, and length of lateral roots/root hairs (Meister et al. 2014; Li et al. 2016; Forde 2014), Meister et al. 2014; Li et al. 2015).

In wheat, due to lack of complete knowledge about the genetic basis of NUE, and associated  $G \times E$  interactions, selection of cultivars with RSA-based NUE has been suggested (Garnett et al. 2009). QTL studies involving all RSA traits (mentioned above) are also available in wheat. Numerous wheat QTLs for NUE traits at physiological and agronomic levels have been reported (Fan et al. 2019; Zhang et al. 2019; Brasier et al. 2020). Similarly, QTLs that regulate RSA have also been identified (Salarpour et al. 2020; Yang et al. 2020). Despite these significant advances in information about the genetics of NUE and RSA, only a very small fraction of these QTLs and the associated markers could be utilized in actual breeding. The reasons for this failure have been widely discussed (Misztal, 2006; Collard and Mackill, 2008; Cobb et al. 2019).

In order to overcome the above limitations in using QTLs for the development of wheat cultivars with higher NUE, a meta-QTL (MQTL) analysis seems to be an appropriate approach, which allows identification of the most robust and stable MQTLs (Goffinet and Gerber, 2000; Veyrieras et al. 2007). These MQTLs have shown to be more effective than QTLs for their use in marker-assisted selection (MAS) because the MQTLs generally have reduced confidence intervals (CIs) and improved

phenotypic variation explained (PVE%). MQTLs have also been shown to be useful for the identification of promising candidate genes (CGs) associated with the trait in question. Improved software and algorithms have become available and are being increasingly utilized for meta-QTL analysis (Sosnowski et al. 2012; de Oliveira et al. 2014). The approach has already been used to identify MQTLs for a variety of traits in all major crops, including wheat (Online Resource 1), rice (Kumar and Nadarajah 2020; Khahani et al. 2020, 2021), barley (Zhang et al. 2017) and maize (Zhao et al. 2018).

Meta-QTL analysis in wheat has already been conducted for a number of traits, which are listed in Online Resource 1. A solitary study on MQTL for traits relevant to NUE was also conducted, almost ten years ago (Quraishi et al. 2011), where 11 MQTLs based on only three studies were reported. Similarly, reports on MQTLs for RSA using QTLs reported till 2017 are also available (Darzi-Ramandi et al. 2017; Soriano and Alvaro, 2019). A large number of studies involving interval mapping for NUE have also been conducted in different crops including wheat during the last 10 years (Online Resource 2). Since hundreds of QTLs for NUE in wheat have been reported during the last decade (after the only report of MQTL for NUE published in 2011), a fresh meta-QTL analysis is warranted. The MQTLs for the same trait have also been used for identification of the so-called ortho-MetaQTLs, which seem to be conserved over cereals and therefore will be more reliable and can be used in more than one cereals. This identification of ortho-MQTLs has been facilitated by a high level of synteny and collinearity between wheat and other cereals.

Keeping in view the above, the present study was planned, which involved meta-analysis for NUE and RSA in wheat and ortho-MQTL analysis involving wheat and maize. For NUE, QTLs reported during 2006–2020, and for RSA, QTLs reported during 2018–2020 were utilized for the present study. Since MQTLs for NUE are also known in maize (Ahn et al. 1993; Bennetzen and Chen, 2008), ortho-MQTLs for wheat and maize were also worked out with the hope that the results of the present study may be used not only for wheat and maize but also for other cereals (due to conserved nature of ortho-MQTLs). MQTLs for NUE/RSA were not available in other cereals like rice, barley, etc. for identification of ortho-MQTLs involving all the cereals in the present study. Results of the meta-analysis were also compared with the available results from GWAS, and integrated with transcriptomics, and rice–wheat orthology to identify the promising genomic regions and important CGs, which affect NUE/RSA in wheat. The findings of the present study should prove useful for the improvement of wheat

cultivars for yield potential, stability, and performance under N-limiting conditions.

## Materials and methods

### Bibliographic search and data collection

A comprehensive bibliographic search was carried out on wheat QTLs related to NUE published during 2006–2020; QTL information associated with RSA traits under different levels of N contents, published during 2018–2020 was also collected. Details on 15 studies for QTLs associated with NUE and 9 studies for QTLs associated with RSA are summarized in Online Resource 2. Each study was utilized for collecting the following information: (i) data on associated traits, (ii) type and size of the mapping population, (iii) position of QTLs (peak position and genetic CI), (iv) LOD (logarithm of the odds) score for each QTL, (v)  $R^2$  or PVE (phenotypic variation explained) for each QTL, (vi) closely linked or flanking markers. Studies with incomplete information were not included.

### Construction of consensus map and QTL projection

Following three high-quality linkage maps containing different types of markers, extensively used in QTL mapping studies, were utilized to prepare a consensus map: (i) 'Wheat\_Composite\_2004' available at GrainGenes database (<http://wheat.pw.usda.gov>), (ii) 'Wheat, Consensus SSR, 2004' (Somers et al. 2004), (iii) the integrated map constructed by Marone et al. (2013). Markers flanking individual QTLs, identified in all 24 QTL mapping studies, were also included on this consensus map. The R package "LP merge" (Endelman and Plomion 2014) was used to construct a consensus map for meta-QTL analysis. Construction of consensus map using LPmerge involves two steps. First, it computes the number of consensus bins, markers, and ordinal conflicts (if available). If there are inconsistencies in the order of markers in the linkage maps, it resolves them by removing ordinal constraints using statistical manipulations. Second, it generates 1 to 4 consensus maps ( $K = 1$  to 4, where  $K$  is the maximum interval size); from which one or more maps can be chosen using the associated statistics developed for this purpose; this is accomplished by estimating the root mean square error (RMSE, based on mean and standard deviation) between each initial map and the consensus map. The final map for further analysis was the consensus map with a length close to the mean length of the component linkage maps associated with the lowest standard deviation.

The QTLs having the following information were selected for projection on the consensus map: (i) PVE, (ii)

LOD scores, (iii) peak positions, and (iv) CIs. For QTLs, lacking original CI, 95% CI was calculated based on population-specific equations derived by Darvasi and Solter, (1997) and Guo et al. (2006). The QTL positions were then projected on the consensus chromosome map utilizing a scaling rule between the marker interval of the QTLs and the corresponding CI on the consensus map (Arcade et al. 2004; Veyrieras et al. 2007). BioMercator v.4.2 (<https://urgi.versailles.inra.fr/Tools/BioMercator-V4>) was used for this purpose. The new CI of each QTL on the consensus map was computed using Gaussian distribution (Veyrieras et al. 2007).

### Meta-QTL analysis and verification using GWAS

After QTL projection, meta-analysis was performed for each chromosome, separately, using BioMercator v.4.2. Since the number of QTLs per chromosome was  $> 10$ , an algorithm, involving two-step analysis, developed by Veyrieras et al. (2007) was used for the analysis. In the first step, five different models (based on the presence of 1, 2, 3, 4, or  $N$  real QTLs) were used, and the best model was defined using Akaike (AIC) statistics. The second step involved setting up suitable parameters for further analysis; these parameters included the actual number of MQTLs or real QTLs to be mapped on the concerned chromosome. The details of statistical approaches and algorithms that are available in the Biomercator software are described in several earlier studies (e.g. de Oliveira et al. 2014). The LOD and PVE values of MQTLs were calculated as averages of LOD and PVE values of the QTLs involved.

The nucleotide sequences of the markers flanking the MQTLs were retrieved either from the published literature or the databases such as GrainGenes (<https://wheat.pw.usda.gov/GG3/>) and CerealDB (<https://www.cerealsdb.uk.net/cerealgenomics/CerealsDB/indexNEW.php>). The retrieved sequences were used for BLAST against the wheat reference genome (RefSeq v1.0) available in EnsemblPlants to identify the physical coordinates of the MQTLs. Physical positions of some SNPs were directly obtained from the JBrowse wheat genome browser (<https://wheat-urgi.versailles.inra.fr/Tools/Jbrowse>).

Information on marker-trait associations (MTAs) for NUE and RSA identified in recent GWA studies was collected and used for a comparison with MQTLs identified during the present study. Similarly, the physical positions of markers (significantly associated with the trait) were obtained either from databases or through BLAST searches. GWAS-MTAs that occurred within 5 Mb physical regions around the MQTLs were considered to be co-located with the MQTLs (Yang et al. 2021).

## Identification and characterization of ortho-MQTLs using wheat and maize MQTLs

Ortho-MQTLs were identified using synteny and collinearity between wheat and maize MQTLs. For this purpose, only robust wheat MQTLs each involving at least 15 initial QTLs were utilized along with available information on maize MQTLs (Guo et al. 2018). In each case, a set of CGs underlying the wheat MQTLs was used for the identification of syntenic regions in maize MQTLs using the EnsemblPlants database.

### Mining of candidate genes and expression analysis

Physical coordinates of MQTLs were utilized for the identification of CGs using the BioMart tool of EnsemblPlants. Only MQTLs with  $\leq 2$  Mb CI were initially considered for identification of available CGs; for other MQTLs, where the physical interval was  $> 2$  Mb, the physical position of the MQTL peak was calculated according to Jan et al. (2021) and then a 2 Mb region around the MQTL peak was used for identification of CGs.

In-silico expression of CGs identified as above was conducted using the Expression Visualization and Integration Platform (expVIP) (<http://www.wheat-expression.com/>); the available relevant transcriptomics datasets were utilized for this purpose (e.g., Ramírez-González et al. 2018). CGs with expression levels  $> 2$  transcripts per million (TPM) in relevant plant parts/tissues (e.g., roots, shoots, leaves, and grains) were considered for further analysis following the criteria suggested by Wagner et al. (2013). For better visualization of the patterns of gene expression, heat maps were generated using an online platform ‘Morpheus’ (<https://software.broadinstitute.org/morpheus/>). CGs with known functions were accepted as high-confidence CGs for individual MQTLs.

### Wheat orthologues for NUE-related rice genes

Basic information on NUE-related rice genes was collected from two recently published research papers (Han et al. 2016; Zhang et al. 2020a, 2020b); protein sequences of these rice genes were extracted from the NCBI database (<https://www.ncbi.nlm.nih.gov/>). Wheat orthologues of these rice genes were identified from the wheat reference genome using extracted proteins sequences for BLASTP searches. The genes found within MQTL regions were accepted as wheat orthologues for NUE traits. These wheat orthologues were subjected to expression analysis utilizing the relevant transcriptomics datasets available at the expVIP. Levels of gene expression were assessed using TPM values, which were then used for developing heat maps.

## Results and discussion

### Salient features of the QTLs

A total of 1,788 QTLs were available from 24 earlier studies, carried out during 2006–2020 (Online Resource 2, 3). These studies involved 20 DH/RIL populations ranging in size from 91 to 227 lines. Some of the essential features of this data include the following: (i) The 1,788 initial QTLs were distributed on all the 21 wheat chromosomes (Fig. 1a). The sub-genome B carried the maximum number of QTLs (721 QTLs) and the D sub-genome carried the minimum (457 QTLs) which is in agreement with previous meta-QTL studies conducted for NUE and RSA in wheat (Quraishi et al. 2011; Darzi-Ramandi et al. 2017; Soriano and Alvaro, 2019). (ii) The number of QTLs per component trait ranged from 77 for enzymatic activities to 602 for agronomic traits (ATs) (Fig. 1b). All the traits associated with NUE and RSA were grouped into 6 main categories (Online Resource 4). (iii) CIs for QTLs ranged from zero to 96 cM, with an average of 10.01 cM (Fig. 1c). (iv) The PVE of individual QTLs ranged from 1.55 to 55.81%, with an average of 10.65% (Fig. 1d). The QTL data collected in this study has been made publicly available through a recently developed WheatQTL database (<http://wheatqtl.db.net/>) (Singh et al. 2021).

### Wheat consensus map

The consensus genetic map included a total of 1,40,166 markers (Online Resource 5, 6) spread over a length of 6853.27 cM, thus giving a density of 20.45 markers/cM for the whole genome. For individual chromosomes, the size of the genetic map ranged from 127.70 (6B) to 661.02 cM (2D) (Fig. 2), the number of markers ranged from 1177 on 4D to 15,716 on 3B and the density of markers ranged from 4.07 markers/cM for 1B to 83.14 markers/cM for 6B (Fig. 2, Online Resource 6). The sub-genome A covered a distance of 2538.18 cM with 61,949 markers (24.41 markers/cM), the sub-genome B covered a distance of 2289.26 cM with 58,846 markers (25.70 markers/cM) and the sub-genome D covered a distance of 2025.82 cM with 19,371 markers (9.56 markers/cM). These features are not very different from those on chromosome maps used in earlier meta-QTL studies (Venske et al. 2019; Jan et al. 2021). The map developed in the present study is much better, relative to those prepared and used in three earlier studies for meta-QTL studies for the traits under study (Quraishi et al. 2011; Darzi-Ramandi et al. 2017; Soriano and Alvaro, 2019).

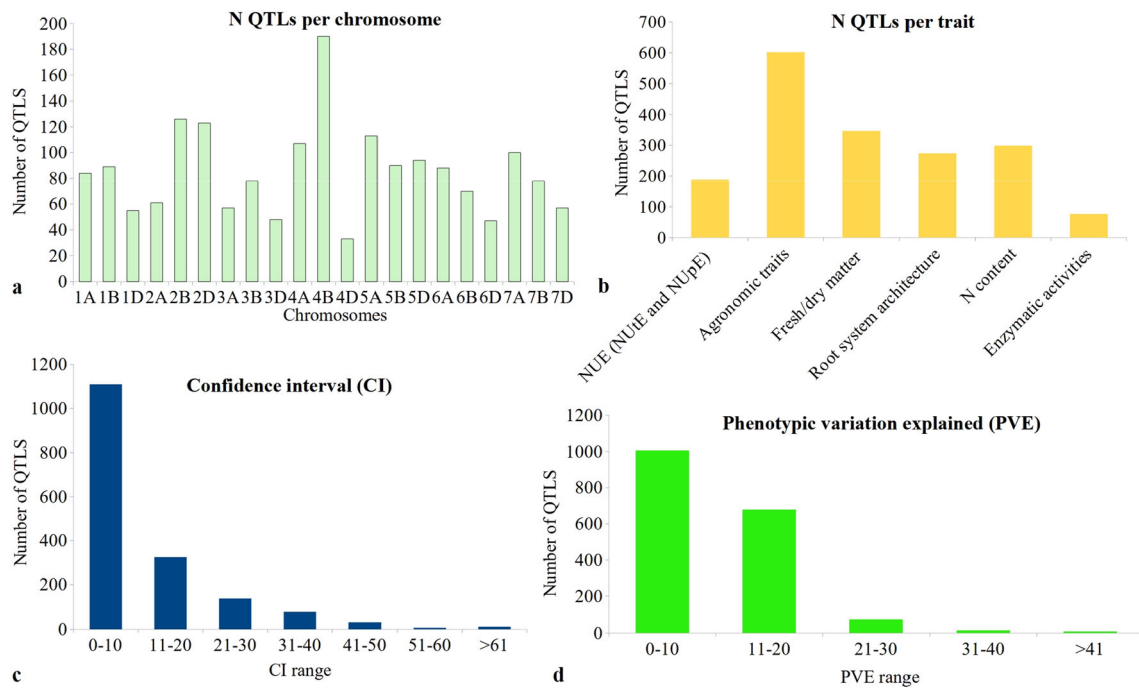
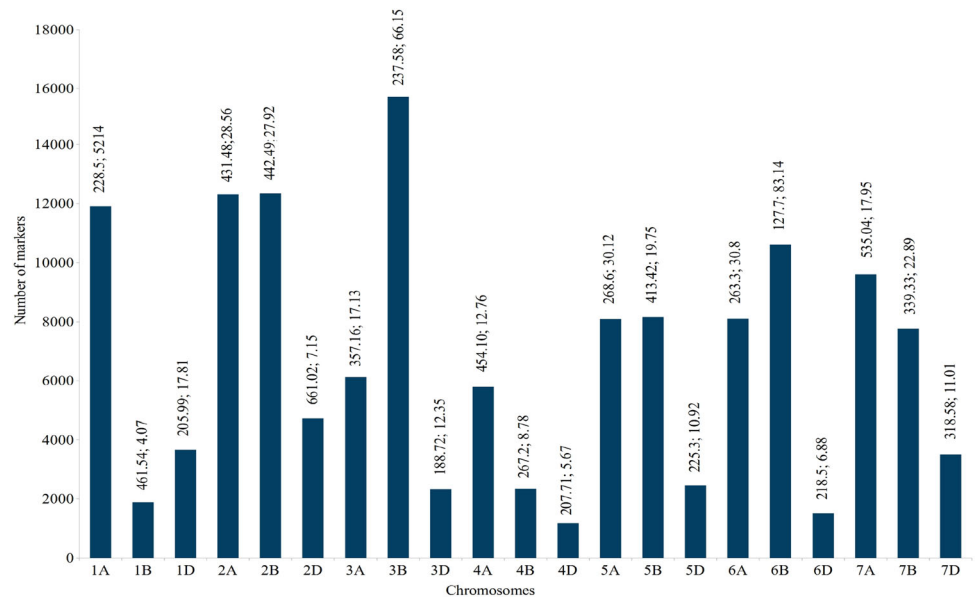


**Fig. 1** Frequencies of QTLs used for identification of MQTLs in wheat, based on four different criteria: **a** number of QTLs for 21 chromosomes arranged according to 7 homoeologous groups (1–7), each group with three sub-genomes (A, B, D), **b** frequencies of QTLs

for each of the six traits, **c** frequencies of QTLs with different size of CI (in cM), and **d** frequencies of QTLs with different levels of phenotypic variation explained (PVE%)

**Fig. 2** Details of the consensus map, showing frequencies of mapped markers on each of the 21 chromosomes; on top of each bar representing individual chromosomes are given length of each chromosome (in cM) and marker density (markers/cM)



**MQTLs for NUE and RSA**

Only 1703 QTLs of the available 1788 QTLs could be used for projection onto the consensus map; the remaining 85 QTLs did not have complete information required for the projection; 118 MQTLs involving 1098 QTLs were identified using meta-QTL analysis (Online Resource 7) (Fig. 3). The remaining 605 QTLs could not be assigned to

any MQTL, since they either lacked common markers between consensus and initial maps, or the QTLs had relatively low  $R^2$  values and/or large CI. The distribution of MQTLs on 21 individual chromosomes was not proportionate to the number of QTLs carried by them. For instance, chromosomes 4B, 5A, 6A, and 7B carried fewer MQTLs and were not proportionate to the density of QTLs on these chromosomes.



**Fig. 3** Distribution of 118 MQTLs on 21 wheat chromosomes. The boxes on the right of each chromosome represent the positions of MQTLs (with name of MQTL in each case) for three different features, (red boxes: GWAS-verified MQTLs, green boxes: breeder’s QTLs, black boxes: un-verified MQTLs). On the left of each bar representing a chromosome, are given distances in cM, and on the right are given pairs of flanking markers for each MQTL

The number of QTLs involved in an individual MQTL varied from 2 to 52 (Fig. 4a); however, the following five MQTLs were each based on > 25 QTLs: MQTL4A.2 (26), MQTL5D.6 (26), MQTL5A.1 (29), MQTL4B.4 (38), and MQTL4B.1 (52). This is in sharp contrast to several earlier studies, where none of the individual MQTLs carried > 18 QTLs (Quraishi et al. 2011; Darzi-Ramandi et al. 2017; Soriano and Alvaro, 2019). Twenty (20) of the 118 MQTLs identified in the present study had genomic locations that overlapped with MQTLs found in at least one of the three previous studies (Darzi-Ramandi et al. 2017; Soriano and Alvaro, 2019; Quraishi et al. 2011) (Online Resource 8); 14 of these 20 MQTLs were also verified using GWAS results. All these verified MQTLs may be used with high confidence for MAS and for further basic studies including positional cloning and functional studies of underlying CGs.

The CI of MQTLs, on an average, was reduced 8.56 fold relative to the CIs in QTLs used (the range of CI in QTLs was 0 to 96 cM with a mean of 10.27 cM), although the average reduction in the size of CI for individual MQTLs widely differed in individual chromosomes and could reach 24.87 fold reduction on chromosome 5D and 40.52 fold reduction on chromosome 4B followed by 19.34 fold in 4D and 15.78 fold in 5A (Fig. 4b). These reductions in the size of CIs are in sharp contrast to those reported in several earlier studies on NUE/RSA, where CI was reduced by

merely 2.98 times (14.8/4.96) in one study (Soriano and Alvaro, 2019) and 3.25 (20.8/6.4) in another study (Darzi-Ramandi et al. (2017).

The MQTLs were anchored to the physical map of the wheat reference genome; for only 6 MQTLs, physical coordinates could not be worked out, since these MQTLs were flanked by markers like AFLP, which did not have any sequence data required for BLAST searches (Online Resource 7). The physical lengths of 112 mapped MQTLs differed with a range of 0.02 Mb for MQTL3A.3 to 666.18 Mb for MQTL1B.7, with a mean of 94.36 Mb (29 of these MQTLs each covered a physical distance of < 2 Mb).

Several MQTLs exhibited a clustered distribution with some overlapping MQTLs within a cluster. This clustering of MQTLs was particularly apparent in chromosome 1A (3 MQTLs within 527.18 to 591.64 Mb region), 1B, (8 MQTLs within 17.32–683.81 Mb), and 2A (3 MQTLs clustered within 25.6–43.3 Mb). Other clusters with some overlapping regions were observed on the following wheat chromosomes: 2B (4.48–41.47 Mb), 4A (601.04–695.53 Mb), 6B (30.25–694.99 Mb), and 7A (2.72–210.63 Mb), etc. (Online Resource 7). Such clustering of MQTLs was also reported in some earlier studies (Jan et al. 2021; Saini et al. 2021; Yang et al. 2021) and is a desirable feature for the transfer of more than one MQTL during MAS. These clusters may prove useful for marker-assisted breeding (MAB).

Individual MQTLs also differed for the number of traits each controlled; the number of traits controlled by an individual MQTL ranged from a solitary trait controlled by MQTL3B.2 to as many as 26 traits controlled by MQTL4B.1. As many as 70 MQTLs out of 118 each carried QTLs for several traits including both NUE and RSA. According to one study, RSA shows a significant positive

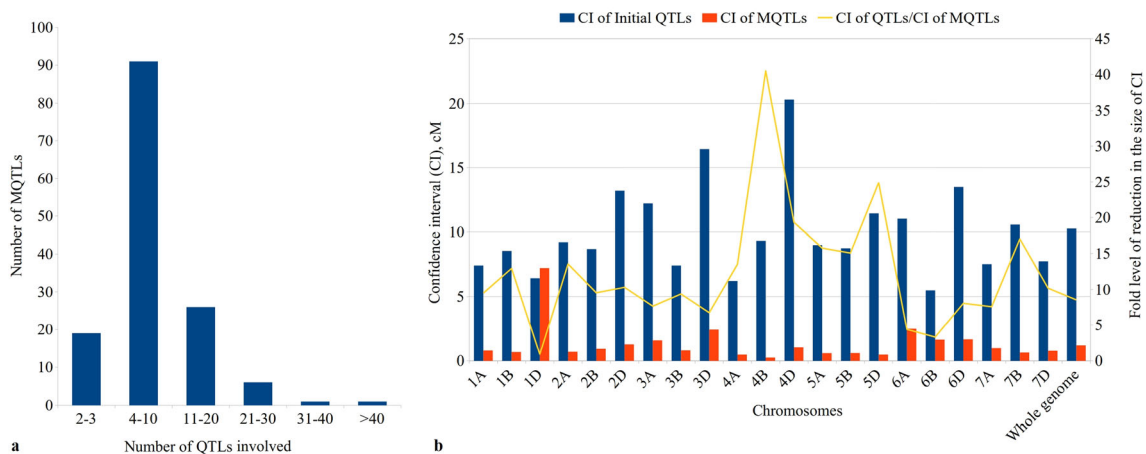


**Fig. 4** Basic information of MQTLs identified, **a** frequencies of MQTLs harbouring different number of QTLs, **b** comparison of CIs of QTLs and those of meta-QTLs, showing fold level of reduction in the size of CI

correlation with NUpE but no correlation with NUE, implying that only N acquisition, not N utilisation, is most probably related to the function of roots (Li et al. 2015; Garnett et al. 2009). The MQTLs were used for a further selection of some promising MQTLs using the following criteria: (a) CI < 2 cM, (b) average PVE > 10%, (c) average LOD > 5, and (d) involvement of at least 10 initial QTLs with the MQTL. This exercise resulted in the selection of 9 promising MQTLs, which we like to call breeder's QTLs; these breeders' QTLs with their essential features are listed in Table 1. All these breeder's QTLs (except MQTL2A.2) involved QTLs for both NUE and RSA, hence, these can be used by breeders for the improvement of both NUE and RSA.

### Comparison of MQTLs with results of GWAS

The physical positions of MQTLs were also used for comparison with MTAs for NUE/RSA reported in earlier GWAS conducted on durum (tetraploid) and bread wheat (hexaploid). Information on MTAs for NUE and RSA identified in 17 GWA studies published during 2017–2021 is available in Online Resource 9. For this purpose, only 112 physically mapped MQTLs could be considered; 88 of these MQTLs each matched one or more known MTAs from among 412 MTAs (Online Resource 10; Table 1) that were available for comparison. Among them, 45 MQTLs were verified using GWAS for durum wheat, and 81 were verified using GWAS for hexaploid wheat (38 MQTLs were verified with both durum and bread wheat).

The number of matching MTAs for each MQTL also differed, so that as many as 21 MQTLs each matched with at least 10 MTAs identified in 17 GWA studies; of these MQTL5B.2 matched with 60 MTAs, followed by MQTL6B.4, 1B.7, and 1B.4 with 55, 49, and 40 MTAs, respectively. Some of the MQTLs (e.g., MQTL1B.2, 1B.3, and 4B.4) each involving 18 or more initial QTLs matched with more than 20 MTAs (Online Resource 10). These MQTLs overlapping MTAs may be used for mining CGs affecting the NUE and RSA traits. The frequency distribution of some GWAS-validated MQTLs is depicted in Fig. 5.

A comparison MQTLs with GWAS-based MTAs, as above, has been undertaken only sparingly in wheat, where two such studies are available (Aduragbemi and Soriano, 2021; Yang et al. 2021). In these two studies, only 38.66% and 61.37% of MQTLs, respectively, could be verified with the GWAS results. These values of MQTLs verified by GWAS in earlier studies seem to be in agreement with our results. One can perhaps speculate about the reasons for the lack of verification of the remaining MQTLs with MTAs from GWAS. The simplest explanation is that none of the studies (meta-QTL analysis and GWAS) covered the entire

genetic variation and that the material used for two sets of studies differed widely.

### Ortho-MQTLs in maize

In order to identify ortho-MQTLs for wheat and maize, the syntenic regions of each of the 19 selected wheat MQTLs were compared with previously published maize MQTLs for a variety of traits (Guo et al. 2018). Another solitary study of MQTLs for NUE in maize (Liu et al. 2012) could not be utilized due to the non-availability of complete data required for such analysis. Nine ortho-MQTLs were identified for RSA, which were located on the following six maize chromosomes: 3, 4, 5, 8, 9, and 10; the number of MQTLs for individual ortho-MQTL ranged 1 to 3. The detailed information on ortho-MQTLs is available in Online Resources 11, and 12.

Ortho-MQTLs in wheat were also studied in two earlier studies (Quraishi et al. 2011; Saini et al. 2021). In one of these studies, an ortho-MQTL associated with NUE was identified for four different related crops including wheat, maize, sorghum, and rice; the study also included the identification of a structurally and functionally conserved gene called glutamate synthase (*GoGAT*) at orthologous locations in these closely related species. Two conserved flanking markers were also developed for the *GoGAT* gene (Quraishi et al. 2011). Such orthologous genes for NUE/RSA can also be identified using the results of the present study for further detailed study. A conserved orthologous set (COS) of markers may also be developed for their use in MAS for cereal breeding programs (Quraishi et al. 2009).

### Candidate genes and their expression analysis

In the genomic regions defined by 112 of the 118 MQTLs, a total of 1991 CGs (Online Resource 13) were found. Several genes/gene families with related functions were detected frequently in different MQTL regions (Fig. 6). These genes included the following: 98 genes encoding proteins containing kinase domain, 79 genes for proteins containing F-box-like domains, 40 genes for cytochrome P450 proteins, 32 genes for glycoside hydrolases, 22 genes for UDP-glucosyltransferases, 16 genes for NAC TFs, 14 genes for expansins, 13 genes for early nodulin-93 proteins, 11 genes for GRAS TFs and 10 genes for ABC transporter-like proteins. (Fig. 6). Association of these genes/gene families with NUE and/or RSA has been reported in several earlier studies (Zhang et al. 2020a, 2020b; Meijón et al. 2014; Jun et al. 2015; Minic 2008; Dong et al. 2020; He et al. 2015; Marowa et al. 2016; Bi et al. 2009; Do et al. 2018). In the present study, some genes that are known to be associated with NUE and RSA appeared in clusters.



**Table 1** A summary of 88 MQTLs for NUE/RSA, (verified using GWAS) with details of flanking markers, QTLs and the traits involved

MQTLs (Phy. interval, in Mb)	Flanking markers (CI in cM)	No. of QTLs involved (avg. LOD)	Traits <sup>b</sup> (avg. PVE)
MQTL1A.1 (574.67–575.01)	AX-110966426/AX-108822131 (13.65–14.31)	6 (3.36)	FSS, SPS, DTM, GY, NU <sub>p</sub> E, GPC (5.77)
MQTL1A.2 (577.47–577.61)	AX-110518076/AX-110430653 (18.85–19.50)	5 (4.78)	RDM, GN, LA, root N/shoot N content, DTH (8.16)
MQTL1A.3 (13.67–13.76)	AX-109408162/AX-108790365 (24.61–24.74)	5 (4.86)	LFW, N/grain, SL, GW, RL (6.24)
MQTL1A.4 (527.18–591.64)	AX-111580764/AX-95629819 (35.45–36.41)	6 (4.34)	SPS, GY, SPS, GNC, PH (6.58)
MQTL1A.5 (32.92–590.25)	BS00011855_51/AX-109867753 (42.41–43.08)	10 (6.88)	Peduncle %N, RNC, BSSPS, GN, NU <sub>p</sub> E, NUE, PH, GW, N/grain (9.12)
MQTL1A.6 <sup>a</sup> (37.5–185.52)	BS00029346_51/Xwmc826 (54.27–55.92)	13 (5.10)	TFW, RFW/SFW, RDM, RL, LEC, SFW, GW, RFW, TDM, SDW (13)
MQTL1B.1 (430.57–565.67)	AX-109514853/AX-108815832 (10.16–11.14)	6 (5.53)	NUE, NU <sub>t</sub> E, GY, PH, DTM, PH (12)
MQTL1B.2 <sup>a</sup> (454.17–622.85)	AX-111122733/AX-94407244 (28.54–29.51)	18 (5.24)	RNC, NU <sub>t</sub> E, RL, SDW, SNC, TDM, PH, NU <sub>t</sub> E, RDM/SDW, RN, RDM (14)
MQTL1B.3 (17.32–551.28)	D_1100879/AX-110474859 (45.81–46.20)	20 (5.19)	Peduncle N, TDM, NU <sub>t</sub> E, FSS, RL, NU <sub>p</sub> E, RDM, SDW, SSS, RNC, LFW, GPC, SPP, GW (10)
MQTL1B.4 (17.39–645)	D_1161821/AX-108743608 (49.22–50.32)	6 (5.27)	FSS, RL, TN, DTH, SSS (8.55)
MQTL1B.5 (643.1–643.56)	AX-89682837/AX-108936977 (51.99–52.56)	6 (4.37)	SPP, RNC, RDM, FSS, SL, RD (7.41)
MQTL1B.6 (466.36–646.19)	AX-86176468/AX-89434674 (54.22–55.03)	3 (3.49)	FSS, SPS, DTH (3.32)
MQTL1B.7 <sup>a</sup> (17.62–683.81)	D_1166057/D_1130437 (59.99–60.35)	14 (5.88)	RL, GPC, Peduncle N, SL, GW, RN (11.18)
MQTL1B.8 (666.06–667.42)	AX-111548801/AX-111507640 (73.95–74.04)	8 (4.22)	RFW, RFW/SFW, GY, GW, RDM/SDW (10)
MQTL1D.2 (7.04–9.34)	AX-95082337/AX-109484943 (43.43–51.54)	9 (5.07)	RV, NUE, TNC, ADM, RDM/SDW, SNC, RL, FSS (13)
MQTL1D.3 (10.66–423.3)	Xwmc336/AX-110711194 (59.72–67.87)	4 (6.22)	ADM, DTH, GW (13)
MQTL2A.2 <sup>a</sup> (25.6–43.3)	D_1061332/AX-110492940 (42.58–43.25)	11 (17.17)	SP, GPC, LFW, SP, GW, SC (16.62)
MQTL2A.3 (25.94–29.89)	AX-110435756/AX-109362948 (46.57–47.92)	2 (4.42)	RD, GN (10.81)
MQTL2A.4 (30.25–30.56)	AX-109298548/AX-111761345 (52.45–52.49)	8 (5.05)	RDW/SDW, RDM, SL, NU <sub>p</sub> E, SPP, GW, GN, SL (11.06)
MQTL2A.5 (4.97–5.48)	AX-111719280/Xgwm636 (80.33–80.61)	7 (3.86)	RN, SP, RL, NU <sub>t</sub> E, leaf GS activity, SL (7.47)
MQTL2B.2 (6.07–6.52)	D_1265806/D_3534443 (14.58–15.89)	8 (3.13)	SDW, ADM, PH, TDM, SFW, NUE, RFW, RDM (8.75)
MQTL2B.3 (4.48–13.75)	S_1675663/S_1105975 (33.27–34.43)	3 (3.56)	GW, Lodging (7.14)
MQTL2B.4 (17.44–37.38)	D_4989699/AX-109364692 (43.54–44.79)	17 (4)	RDM/SDW, NU <sub>t</sub> E, RNC, TDM, GW, SNC, SPP, leaf GS activity, SL, LEC, Peduncle %N, SP (10.9)
MQTL2B.5 (17.17–41.47)	Xwmc597/tPt-4627 (47.81–49.87)	5 (3.85)	RN, SPS, SC, GY, TNC (7.15)
MQTL2B.6 (22.61–24.11)	D_2278188/D_1004475 (59.88–60.53)	8 (4.77)	SDW, SFW, DTH, RN, FSS, SC, TDM, StNC (8.88)

**Table 1** continued

MQTLs (Phy. interval, in Mb)	Flanking markers (CI in cM)	No. of QTLs involved (avg. LOD)	Traits <sup>b</sup> (avg. PVE)
MQTL2B.7 (24.9–31.38)	<i>D_1241419/D_1137511</i> (78.14–78.93)	7 (4.8)	Peduncle N, RL, RN, GW, N/grain, SL (7)
MQTL2D.1 (475.46–527.38)	<i>D_1159406/D_995055</i> (52.46–53.42)	7 (9.82)	SRA, PH, ADM, NUE, DTH (18.12)
MQTL2D.5 (201.38–374.63)	<i>D_1159229/D_3936747</i> (91.83–92.52)	8 (5)	StNC, GY, GPC, GW, SSS, SC, DTH, RL, FSS (10.77)
MQTL2D.6 (121.39–203.82)	<i>D_1282387/D_2244257</i> (98.47–101.75)	13 (3.57)	FSS, SSS, NU <sub>p</sub> E, RDM, SC, SL, PH, SPS, RV, SL (13.23)
MQTL3A.1 (17.37–17.37)	<i>Xwmc11/D_1288694</i> (23.4–24.98)	10 (5.27)	RD, LFW, RV, SPS, SSS, DTH, GW, RL (6.23)
MQTL3A.2 (25.94–29.05)	<i>AX-111265814/D_2263154</i> (47.48–49.43)	7 (5.27)	RL, NUE, FSS, SPS, LFW, RN (9.23)
MQTL3A.3 (731.07–731.08)	<i>AX-109399066/AX-99469873</i> (70.28–71.91)	16 (4.54)	leaf GS activity, RDM, SL, RL, SSS, SPS, FSS, RD, GW, FSS, HI, SC, TN (8.87)
MQTL3A.4 (690.78–721.22)	<i>wPt-9422/Xwmc169</i> (118.48–120.56)	9 (3.73)	SFW, TNC, SNC, RNC, GW, RL (11.48)
MQTL3A.5 (483.74–595.95)	<i>AX-110000809/S_1005033</i> (197.56–198.26)	3 (13.5)	RDM, RFW/SFW, RDM/SDW (25.53)
MQTL3B.1 (22.91–46.26)	<i>S-1160118/D_1104851</i> (22.11–22.68)	4 (3.65)	RN, Lodging, NU <sub>t</sub> E (9.38)
MQTL3B.2 (747.8–786.97)	<i>Excalibur_c5309_286/D_3025080</i> (31.64–32.24)	2 (3.74)	NUE (8.11)
MQTL3B.3 (434.05–751.21)	<i>D-1403622/D-2290447</i> (39.45–40.96)	10 (4.29)	PH, LEC, SPS, GN/ear, RFW, FSS, DTH, RDM, NU <sub>t</sub> E (5.45)
MQTL3B.4 (700.78–726.62)	<i>D-3385391/D-1085695</i> (53.94–54.6)	8 (4)	RDM/SDW, RFW/SFW, PH, DTH, ADM, GY, RL (10.14)
MQTL3B.5 (670.19–681.52)	<i>D_3021719/D_1106812</i> (61.39–62.2)	5 (5)	GN, SDW, RDM, NUE, Grain N/ear (7.42)
MQTL3B.6 (43.68–479.89)	<i>D-1289877/Xwmc78</i> (73.21–74.09)	5 (3.76)	TDM, RFW/SFW, total N, GPC, FSS, RD (8.49)
MQTL3B.7 (252.34–321.78)	<i>D-1133674/D-1107825</i> (77.53–78.48)	4 (5)	SRA, RN, DTH, NU <sub>p</sub> E (7.38)
MQTL3B.8 (725.18–730.74)	<i>AX-109275917/AX-110380092</i> (104.85–105.18)	6 (4.38)	RDM/SDW, SRA, SDW, RDM, RFW/SFW (9.88)
MQTL3D.2 (427.95–497.95)	<i>wPt-666738/AX-109884133</i> (30.43–31.83)	2 (4.68)	DTM, RD (11.81)
MQTL3D.3 (295.55–516.87)	<i>AX-110687174/MK9974</i> (40.72–40.91)	6 (5.59)	GY, Peduncle N, SPP, RV, RN, RS (9.95)
MQTL3D.5 (560.64–603.71)	<i>Xcfd64/AX-108969398</i> (69.11–70.41)	8 (3.56)	GN, NGA, GY, GPC (6.55)
MQTL4A.1 (691.14–694.9)	<i>Xwmc262/Xbarc343</i> (18.68–19.61)	12 (4.49)	SNC, TNC, NUE, HI, DTH, RNC, NU <sub>t</sub> E (16.78)
MQTL4A.2 <sup>a</sup> (651.78–695.53)	<i>D_1054130/S_1242937</i> (33.64–33.88)	26 (12)	RFW, NU <sub>p</sub> E, RDM, DTH, RFW/SFW, NU <sub>t</sub> E, RD, RNC, HI, SPS, TFW, SL, ADM, SPP, SFW, FSS, NUE (23.78)
MQTL4A.3 (616.89–647.84)	<i>AX-111670204/D_1051322</i> (45.94–46.59)	22 (6.53)	LEC, NU <sub>t</sub> E, NUE, SL, N/grain, Peduncle %N, SSS, SRA, GN, RFW/SFW, NU <sub>p</sub> E, PH, Grain N/ear, RFW, GW, SP, RL, LFW, GS activity/leaf, Grain %N (9.53)
MQTL4A.4 (622.17–657.2)	<i>D_1053244/AX-111710911</i> (56.58–57.49)	6 (3.85)	HI, RDM, RDM/SDW, GN, TDM, TFW (9.78)

**Table 1** continued

MQTLs (Phy. interval, in Mb)	Flanking markers (CI in cM)	No. of QTLs involved (avg. LOD)	Traits <sup>b</sup> (avg. PVE)
MQTL4A.5 <sup>a</sup> (633.36–678.04)	<i>AX-110037196/D-3026871</i> (66.48–66.51)	17 (5.16)	RL, RN, NUE, RDM, SNC, RNC, RL, TDM, PH, SDW (10.91)
MQTL4A.6 (601.04–691.14)	<i>Xwmc513/</i> <i>RAC875_rep_c108054_95</i> (69.51–69.96)	8 (4.41)	RL, DTH, SL, TFW, SFW, NUE (8.9)
MQTL4B.1 <sup>a</sup> (576.5–657.27)	<i>D_2265275/S_2318924</i> (72.51–72.82)	52 (6.73)	GW, GN, FSS, DTH, SPP, total N, NGA, StNC, PH, GY, GPC, Grain N/ear, ADM, SPS, RV, Peduncle %N, GFD, NUE, SL, TDM, NUE, SDW, RL, RDM, GW, NUpE (10.49)
MQTL4B.2 <sup>a</sup> (179.02–530.53)	<i>S_5412102/D_1027953</i> (81.27–81.42)	15 (5.69)	NUE, GW, SL, ADM, SNC, RDW/SDW, TDM, SDW, SPP, RN, RL (11.5)
MQTL4B.3 (104.94–530.53)	<i>D_1027953/D_1109164</i> (84.62–85.07)	5 (9)	NUE, GN, TNC, root N/shoot N content (18.23)
MQTL4B.4 (104.94–627.44)	<i>Xbarc60/D_1109164</i> (87.18–87.18)	38 (4.69)	NUE, GN, SL, PH, GW, NGA, GPC, ADM, GNC, SWPP, BSSPS, SPP, SPS, root N/shoot N content, SNC, HI, RDW/SDW, TDM, SDW (10)
MQTL4D.2 (484.66–494.84)	<i>Xwmc399/AX-109334705</i> (75.76–76.18)	3 (4)	NUE, RNC, SPP (8.26)
MQTL5A.1 (678.2–680.23)	<i>AX-108732112/AX-109541910</i> (78.32–79.46)	29 (6.42)	SC, GW, SP, SSS, GY, SPP, SL, StNC, SFW, leaf GS activity, RDM, LEC, SPS, Peduncle %N, LFW, DTH, grain N/ear, (9.52)
MQTL5A.2 (689.19–689.62)	<i>AX-109859146/AX-108910506</i> (85.99–85.99)	16 (3.14)	StNU, SC, GY, straw yield, NUE, PH, GNC, NUtE, TNC, SNC, ADM, GW (7.43)
MQTL5B.1 (8.93–13.16)	<i>AX-111536293/AX-111170049</i> (24.89–25.97)	3 (3.82)	GW, RN (7.18)
MQTL5B.2 (10.27–241.26)	<i>AX-110433617/D-1405540</i> (32.91–33.25)	8 (4.77)	SPP, SL, RN, SRA, RD, RV, RDM/SDW (9.24)
MQTL5B.3 (23.33–34.54)	<i>AX-110675968/Xwmc149</i> (51.81–52.45)	14 (5.12)	RFW/SFW, N/grain, SL, NUpE, SC, TNC, SSS, GW, FSS, SP, Peduncle N (9.16)
MQTL5B.5 (55.39–69.13)	<i>AX-110612519/AX-109473183</i> (63.33–64.53)	11 (4.56)	GW, SP, RD, GW, DTH, SRA, PH, RD, SC (7.52)
MQTL5D.6 <sup>a</sup> (266.06–374.26)	<i>Xwmc608/D_3948828</i> (62.37–62.4)	26 (11)	Peduncle N, GFD, SP, Grain %N, LEC, RDM, SL, FSS, TFW, RN, SPS, DTH/M, SSS, Lodging, PH, NUpE, StNC, SDW, TDM, SFW, RFW (12)
MQTL6A.1 (15.94–19.6)	<i>AX-109274358/AX-109856662</i> (45.82–48.81)	22 (5)	GW, ADM, NUpE, GY, TNC, SC, NUtE, SNC, HI, FSS, SRA, StNC, ADM, LEC, RDM/TDM (9.43)
MQTL6B.1 (150.29–591.18)	<i>Xgwm361/AX-108725475</i> (3.89–6.01)	7 (7.31)	PH, RS, GW, TDM, RDM, SL, SP (11.16)
MQTL6B.2 (492.61–653)	<i>AX-109440201/AX-110594295</i> (6.78–8.86)	12 (10)	RN, StNC, PH, GW, SPP, grain N/ear, NUpE, N/grain, Peduncle N, RDM, DTH (13.86)
MQTL6B.3 (470.81–694.99)	<i>S-1054930/Xbarc18</i> (21.28–23.41)	5 (4.92)	StNC, GW, SL, RL, RD (11)
MQTL6B.4 (30.25–596.18)	<i>Xwmc417/Xgwm963</i> (29.79–32.01)	6 (5.07)	leaf GS activity, RS, RV, RL, SPS, GY (11.45)
MQTL6B.5 (375.5–666.28)	<i>D-1270032/AX-108981289</i> (40.72–41.91)	9 (3.9)	RL, FSS, SPS, GW, SRA, SSS (8.12)
MQTL6B.6 (125.54–149.17)	<i>Xwmc104/S-1276135</i> (46.81–46.98)	3 (5.08)	RNC, SL, SRA (6.30)
MQTL6D.1 (0.06–1.57)	<i>Xpsp3200/AX-111503712</i> (0–0.49)	2 (5.61)	NUtE, FSS (11.69)
MQTL6D.2 (7.28–7.71)	<i>AX-108726481/AX-109882824</i> (10.37–11.88)	7 (5.15)	N/grain, RS, GW, RL, SRA, RD, SNC (7.47)
MQTL6D.3 (16.39–26.4)	<i>D-1208709/D-1243222</i> (33.68–38.13)	3 (6.43)	GW, GN/ear, grain N/ear (12.29)
MQTL6D.4 (469.39–472.15)	<i>Xfba85a/Xbarc24</i> (50.4–53.03)	4 (6.25)	GW, RL, SRA (8.32)

**Table 1** continued

MQTLs (Phy. interval, in Mb)	Flanking markers (CI in cM)	No. of QTLs involved (avg. LOD)	Traits <sup>b</sup> (avg. PVE)
MQTL6D.5 (129.49–472.15)	<i>Xwmc113/Xbarc146</i> (58.13–59.5)	2 (3.45)	RL, SL (9.74)
MQTL6D.6 (79.95–129.49)	<i>Xbarc146/Xgwm325</i> (63.68–64.25)	8 (6.32)	grain N/plant, GW, leaf GS activity, SC, RL, SL (11.95)
MQTL6D.7 (97.82–117.36)	<i>Xwmc822/Xgpw304</i> (76.17–76.38)	4 (3)	NUtE, GY, ADM (9.25)
MQTL7A.1 (9.75–10.09)	<i>S_1000950/D_1208529</i> (12.44–13.56)	3 (4.23)	HI, SL, NUE (7.81)
MQTL7A.3 (23.23–26.57)	<i>AX-109938650/AX-108779571</i> (30.4–31.15)	5 (9.89)	NUE, SPS, FSS, LFW (5.55)
MQTL7A.4 (17.33–26.31)	<i>D_1217265/D_4405207</i> (40.72–42.25)	13 (4.35)	SRA, FSS, RN, GY, NUtE, RNC, PH, LEC, TDM (8.89)
MQTL7A.5 (26.31–36.65)	<i>D_1100222/AX-111761655</i> (45.49–46.32)	7 (3.76)	SNC, TNC, SRA, FSS, SDW, RFW/SFW, GY (8.20)
MQTL7A.6 (43.45–210.63)	<i>wPt-7113/wPt-9496</i> (57.12–58.82)	8 (5.57)	RFW/SFW, GN, DTH, GW, grain %N, PH, SNC (8.7)
MQTL7A.7 (15.08–47.44)	<i>S_1124198/AX-111761577</i> (63.74–64.27)	10 (5.06)	leaf GS activity, SP, SDW, TDM, RD, TNC, RDM, RD, FSS (9.4)
MQTL7B.2 (414.81–736.87)	<i>D-1100569/AX-109277778</i> (69.77–71.14)	12 (4.56)	GW, NUtE, TNC, RNC, TDM, SDW, StNC, RDM, DTM, PH (11.7)
MQTL7B.3 (718.19–733.8)	<i>D-1061740/Xfbb226.1</i> (88.29–88.31)	16 (4.49)	GW, NUtE, GN, NUE, RL, RDM/SDW, TDM, SSS, RFW/SFW, RDM, DTH (9.58)
MQTL7D.1 (5.99–8.23)	<i>wPt-743790/Xwmc506</i> (21.67–22.08)	7 (4.39)	RL, SPS, NUtE, GNC, DTM, RN (11.27)
MQTL7D.3 (18.4–89.83)	<i>AX-109353584/D_2291069</i> (47.77–48.72)	9 (6.62)	LFW, NUE, HI, PH, SP, DTH, GW, leaf GS activity (9.19)
MQTL7D.7 (116.69–256.75)	<i>D_1110200/D_1401510</i> (96.51–96.57)	4 (11.45)	SSS, GW, FSS, RFW/SFW (20)

<sup>a</sup>Breeder's QTLs, <sup>b</sup>Traits: FSS fertile spikelet per spike, SPP spikes per plant, SSS sterile spikelets per spike, SPS spikelets per spike, SL spike length, BSSPS bottom sterile spikelet per spike, SC spike compactness, TDM total dry matter, RDM root dry matter, ADM aerial dry matter, SDM shoot dry matter, RDM/SDM ratio of root and shoot dry matter, RUE radiation use efficiency, GNC grain N concentration, SNC shoot N content per plant, RNC root N content, TNC total N content, SP soluble protein, GPC grain protein content, LFW leaf fresh weight, TFW total fresh weight, SFW shoot fresh weight, NUtE nitrogen uptake efficiency, NUtE nitrogen utilization efficiency, GY grain yield, GW grain weight, GFD grain filling duration, DTH/F/M days to heading/flowering, and maturity, TN tiller number, PH plant height, GN grain number, RFW root fresh weight, RFW/SFW shoot fresh weight, LEC leaf extract colour, LA leaf area, SWPP straw weight per plant, RL root length, RN root number, RV root volume, RSA root surface area, SRA seminal root angle, and RD root diameter

These clusters may prove useful for marker-assisted breeding (MAB). These genes belonged to the following classes: (i) protein kinase-like domain superfamily (Yang et al. 2020), (ii) F-box-like domain superfamily (Meijón et al. 2014), (iii) expansins (Marowa et al. 2016), (iv) glutathione S-transferase (Dalton et al. 2009), (v) zinc finger C<sub>2</sub>H<sub>2</sub>-type (Han et al. 2020), and (vii) cytochrome P450 (Xu et al. 2015), etc. (Online Resource 13).

The in-silico expression analysis of the CGs permitted identification of 930 CGs (belonging to 89 MQTLs), with at least 2 TPM, and 307 CGs with more than 5 TPM expressions in different plant tissues; these CGs could be classified in the following two classes based on their

expression patterns: (i) Class I genes, mostly expressed in roots and shoots/leaves tissues at the vegetative stages, suggesting their roles in the regulation of NUtE (Zhang et al. 2020a, 2020b; Han et al. 2016); (ii) Class II genes, mainly expressed in the spike (including rachis, stamen, pistil, stigma, and ovary, etc.) and grains (including endosperm, embryo, seed coat, and aleurone layer, etc.). The genes of class II are generally involved in regulating NUE and in turn affecting grain yield and related traits (Mosleth et al. 2015; Karunaratne et al. 2020) (e.g., Online Resource 14). Some CGs encoding uncharacterized or unpredicted proteins also exhibited significant expression in different plant tissues. These genes should be

**Fig. 5** Frequencies of known GWAS-based MTAs which matched each of 21 MQTLs; for either of the two different traits (NUE, RSA); MQTLs with at least 10 MTAs are included in this figure. MTA results from GWAS using 17 different natural populations were used for this purpose

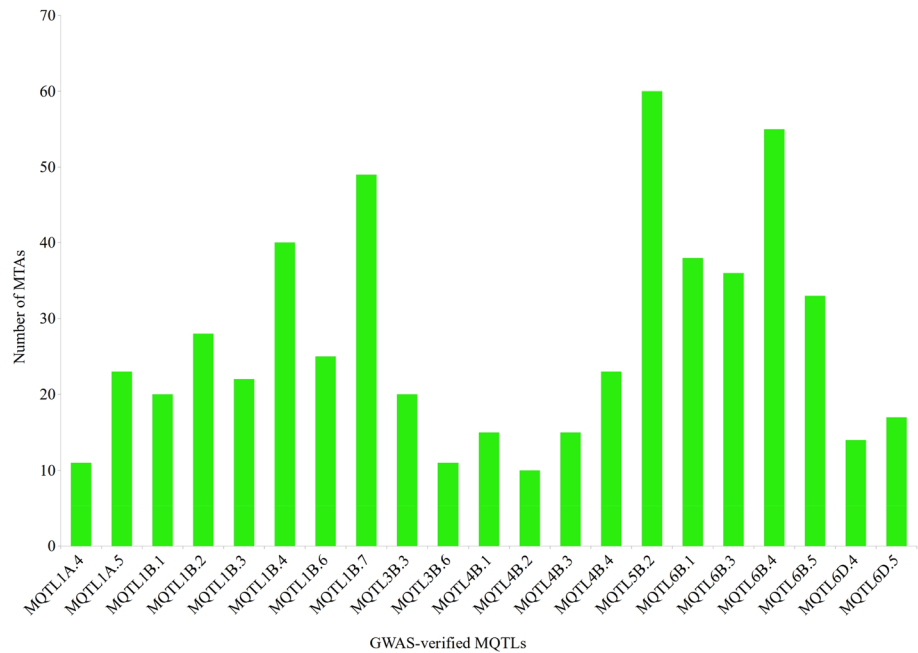
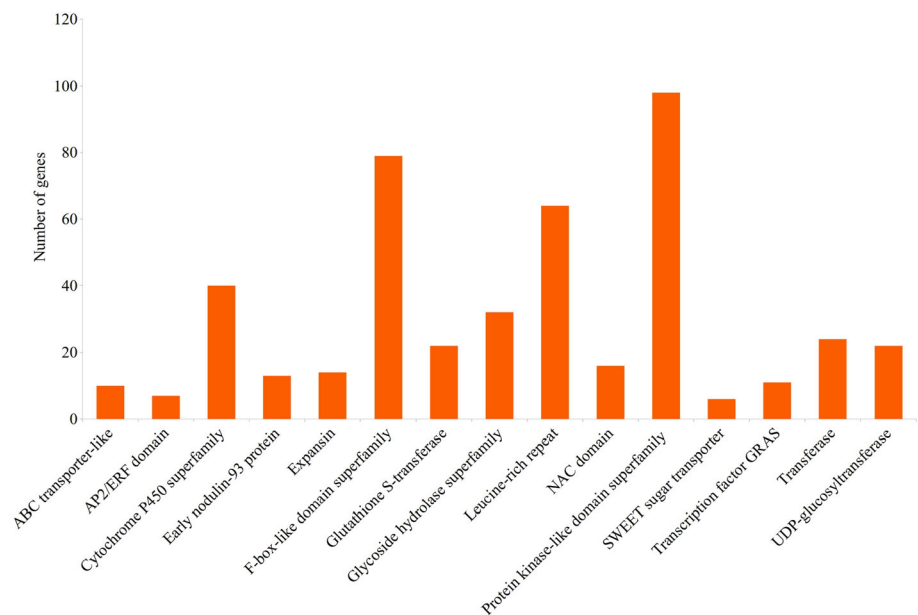


**Fig. 6** Frequencies of candidate genes encoding each of 15 different proteins associated with NUE/RSA



investigated further to see if they play a role in the regulation of NUE in wheat. The expression pattern of some CGs expressed in roots, and shoots/leaves are shown in Fig. 7.

As many as 97 high confidence CGs were detected using the following criteria (i) significant expression in relevant tissues, and (ii) functions previously reported to be important for traits related to either NUE or RSA (Table 2). The molecular and biological functions of these CGs can be studied by cloning/characterization and transgenic approaches. A meta-analysis conducted for three major crops (wheat, rice, and maize) using the data collected from

130 independent genetic transformation studies indicated a promising potential of genetic transformation strategies for improving different NUE parameters (Li et al. 2020).

**Orthologues of rice genes in wheat MQTL regions**

Efforts were also made to find if the wheat MQTLs identified during the present study carry genes that are orthologues of known NUE/RSA genes from other cereals, since synteny and collinearity between wheat genome and genomes of other cereals are widely known now (Gaut, 2002; Kumar et al. 2009). This became possible due to the

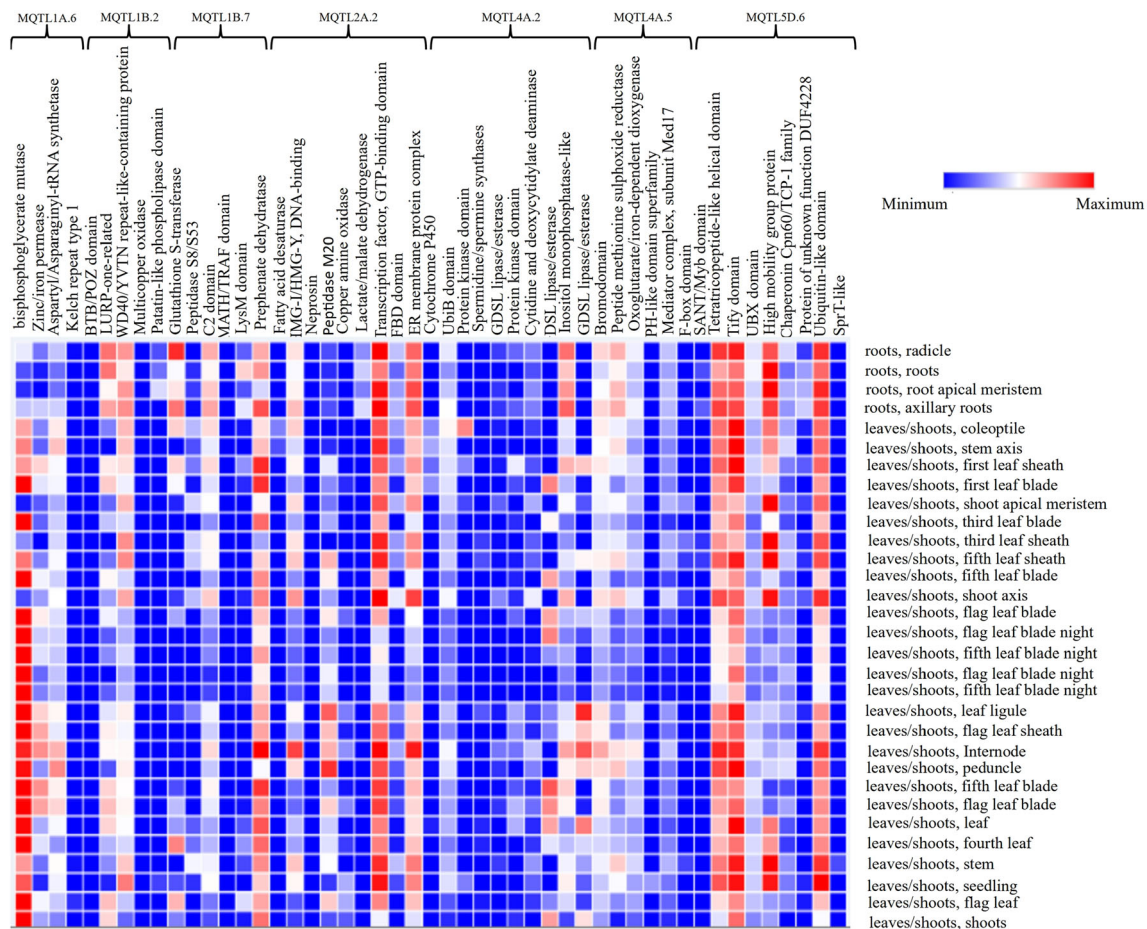


**Fig. 7** Heat map exhibiting levels of differential expressions of important proteins encoded by candidate genes underlying the following 7 MQTLs: MQTL1A.6, MQTL1B.2, MQTL1B.7, MQTL2A.2, MQTL4A.2, MQTL4A.5, and MQTL5D.6; names of proteins encoded by genes are given on the top X axis of the heat map

availability of results from the following studies: (i) In several crops including rice, the molecular basis of NUE or its associated phenotype has been examined using several forward and reverse genetics approaches (Hu et al. 2016; Sun et al. 2021; Xiang et al. 2021; Yu et al. 2021; Zhang et al. 2020a, 2020b). (ii) In rice, some of the important classes of genes involved or implicated in NUE include kinases, transporters, and transcription factors (TFs) (Vidal et al. 2020; Zhang et al. 2020a, 2020b). (iii) Recently, Kumari and Raghuram (2020) and Kumari et al. (2021) compiled a comprehensive list of phosphatases involved in the N-response and/or NUE in crops, and the genes encoding for transporters, TFs, microRNAs, kinases, and phosphatases. They also confirmed differential expression of some promising NUE-candidate genes in a tissue/stage-specific manner through in silico expression analysis (Kumari et al. 2021). The functional studies of many more genes particularly in rice have made it possible to identify orthologues of these genes in complex genomes of related

and the names of 31 classes of organs, where expression of each protein was studied are shown on the left on Y-axis. The scale drawn on the upper right of the heat map represents the range of expression shown by different intensities of blue and red colours

species, including wheat (Han et al. 2016; Zhang et al. 2020a, 2020b). Several crucial genes affecting the NUE of rice have already been reported to have similar functions in wheat, such as *TaNfya-B1*, *AlaAT*, *TaASN2-1A*, *TaGS1.1-4A*, *TaASN2-1B*, *TaGDH1-5A*, *TaNRT2.1*, and *TaNRT2.4-6A* (Qu et al. 2015; Tiong et al. 2021; Karunaratne et al. 2020), which suggests that analysis of homology between related species can be used to select relevant Cgs.

For the present study, 60 rice genes were available (Online Resource 15); 35 of these genes could be utilized for the identification of 49 wheat orthologues in MQTL regions identified during the present study. Of these 35 genes, 18 genes showed more than one wheat orthologue, whereas 17 genes showed only one orthologue in wheat MQTL regions (Table 3). In some cases, orthologues of more than one gene were detected within the same MQTL region. For instance, the three MQTLs, namely MQTL1A.5, 1B.3, and 6D.5 carried orthologues of 8, 5, and 4 different rice genes, respectively. The wheat

**Table 2** High confidence candidate genes (CGs) identified during the present study, with details of MQTLs used, gene IDs extracted from whole genome sequence and the descriptions of related functions (the criteria for identification of these CGs are described in the text)

MQTLs (total number of CGs)	Gene ID for CG	Function description
MQTL1A.1 (4)	TraesCS1A02G416600	Transcription elongation factor 1
MQTL1A.4 (27)	TraesCS1A02G392000	Photosystem I PsuH
	TraesCS1A02G392200	Transcription factor TGA like domain
MQTL1A.5 (7)	TraesCS1A02G174500	Tetraspanin
	TraesCS1A02G174700	Remorin
MQTL1A.6 (4)	TraesCS1A02G110900	Phosphoglycerate/bisphosphoglycerate mutase
	TraesCS1A02G111100	Aspartyl/Asparaginyl-tRNA synthetase
MQTL1B.1 (11)	TraesCS1B02G286300	Cytochrome P450
	TraesCS1B02G286600	G10 protein
MQTL1B.2 (10)	TraesCS1B02G313700	WD40/YVTN repeat-like-containing domain superfamily
	TraesCS1B02G314000	LURP-one-related
MQTL1B.4 (22)	TraesCS1B02G184100	RlpA-like domain superfamily
	TraesCS1B02G184500	Peptidase S10, serine carboxypeptidase
MQTL1B.5 (7)	TraesCS1B02G420300	Transcription factor TGA like domain
	TraesCS1B02G420100	Photosystem I PsuH
MQTL1B.6 (20)	TraesCS1B02G330400	Plant peroxidase
MQTL1B.7 (10)	TraesCS1B02G195800	Prephenate dehydratase
	TraesCS1B02G194900	Glutathione S-transferase
MQTL1B.7 (16)	TraesCS1B02G447300	Leucine-rich repeat domain superfamily
MQTL2A.2 (14)	TraesCS2A02G075500	Fatty acid desaturase
MQTL2A.3 (27)	TraesCS2A02G061600	Glycoside hydrolase family 10 domain
	TraesCS2A02G064600	Zinc finger, PHD-type
MQTL2A.4 (8)	TraesCS2A02G069100	Leucine-rich repeat
MQTL2A.5 (5)	TraesCS2A02G013000	Cytochrome P450
MQTL2B.2 (17)	TraesCS2B02G011700	Gibberellin regulated protein
	TraesCS2B02G012600	START-like domain superfamily
MQTL2B.3 (29)	TraesCS2B02G017700	Cytochrome P450
	TraesCS2B02G019500	Zinc finger, RING-type
MQTL2B.4 (40)	TraesCS2B02G055700	SWEET sugar transporter
	TraesCS2B02G058200	Amine oxidase
MQTL2B.5 (24)	TraesCS2B02G060900	ABC transporter-like
	TraesCS2B02G062900	Transcription factor, TCP
	TraesCS2B02G047000	NAD(P)-binding domain superfamily
MQTL2B.6 (37)	TraesCS2B02G049200	Thiolase
MQTL2D.1 (6)	TraesCS2D02G392800	Oxoglutarate/iron-dependent dioxygenase
	TraesCS2D02G393200	Transcription factor GRAS
MQTL2D.6 (12)	TraesCS2D02G207800	Zinc finger, CCCH-type
	TraesCS2D02G208000	Homeobox-like domain superfamily
MQTL3A.1 (17)	TraesCS3A02G030700	Glycosyltransferase 61
	TraesCS3A02G032200	Zinc finger, RING-type
MQTL3A.3 (24)	TraesCS3A02G511000	F-box-like domain superfamily
MQTL3B.3 (10)	TraesCS3B02G376800	Expansin
	TraesCS3B02G376600	Ribosomal protein S5
MQTL4A.2 (24)	TraesCS4A02G398300	Spermidine/spermine synthases
MQTL4A.3 (23)	TraesCS4A02G359500	SBP domain
	TraesCS4A02G358800	Cytidine and deoxycytidylate deaminase domain
MQTL4A.5 (11)	TraesCS4A02G378300	Oxoglutarate/iron-dependent dioxygenase
MQTL5B.5 (9)	TraesCS5B02G055900	Glutathione S-transferase

**Table 2** continued

MQTLs (total number of CGs)	Gene ID for CG	Function description
	TraesCS5B02G056700	Protein kinase domain
MQTL5B.6 (6)	TraesCS5B02G216500	Zinc finger C2H2-type
	TraesCS5B02G216600	CBS domain
MQTL5D.6 (11)	TraesCS5D02G210900	SANT/Myb domain
	TraesCS5D02G211900	Ubiquitin-like domain
MQTL6A.1 (23)	TraesCS6A02G036100	Peptidase S10, serine carboxypeptidase
	TraesCS6A02G037800	Nin one binding (NOB1) Zn-ribbon-like
MQTL6B.1 (2)	TraesCS6B02G230200	Short-chain dehydrogenase/reductase
	TraesCS6B02G230300	60S ribosomal protein
MQTL6B.2 (14)	TraesCS6B02G323800	Methyltransferase type 11
	TraesCS6B02G324400	Small GTP-binding protein domain
	TraesCS6B02G323400	B-box-type zinc finger
MQTL6B.3 (15)	TraesCS6B02G331300	Glycoside hydrolase
	TraesCS6B02G332400	Zinc finger, RING-type
MQTL6B.4 (1)	TraesCS6B02G220300	Myc-type, basic helix-loop-helix domain
MQTL6B.5 (10)	TraesCS6B02G289600	Glycosyl transferase
	TraesCS6B02G289500	Zinc finger, RING-type
MQTL6B.6 (10)	TraesCS6B02G139100	GDSL lipase/esterase
	TraesCS6B02G139400	F-box domain
MQTL6D.1 (17)	TraesCS6D02G001000	Protein kinase domain
	TraesCS6D02G001600	S-phase kinase-associated protein 1-like
MQTL6D.2 (43)	TraesCS6D02G016700	Glutathione S-transferase
	TraesCS6D02G017000	GTP binding domain
MQTL6D.3 (24)	TraesCS6D02G045500	S-phase kinase-associated protein 1-like
	TraesCS6D02G047000	F-box-like domain superfamily
MQTL6D.4 (42)	TraesCS6D02G400800	Zinc finger, RING/FYVE/PHD-type
	TraesCS6D02G402600	Protein kinase domain
	TraesCS6D02G402800	Zinc finger, CCCH-type
MQTL6D.5 (7)	TraesCS6D02G212800	Senescence regulator S40
MQTL6D.6 (14)	TraesCS6D02G135800	Glucose-6-phosphate dehydrogenase
	TraesCS6D02G136200	WRKY domain
MQTL6D.7 (14)	TraesCS6D02G138000	SWEET sugar transporter
	TraesCS6D02G138200	Oxoglutarate/iron-dependent dioxygenase
MQTL7A.1 (4)	TraesCS7A02G024900	EamA domain
MQTL7A.4 (19)	TraesCS7A02G046200	leucine-rich repeat
	TraesCS7A02G048100	Cytochrome P450
MQTL7A.5 (30)	TraesCS7A02G062600	GDSL lipase/esterase
	TraesCS7A02G064200	Cytochrome P450
MQTL7B.2 (5)	TraesCS7B02G323600	Zinc finger, GATA-type
MQTL7B.3 (27)	TraesCS7B02G469000	cytochrome P450
	TraesCS7B02G469200	Expansin
MQTL7D.1 (52)	TraesCS7D02G000400	Zinc finger, RING-type
	TraesCS7D02G004200	GDSL lipase/esterase
	TraesCS7D02G004400	Acyl-CoA oxidase
	TraesCS7D02G008700	Glycoside hydrolase
MQTL7D.2 (32)	TraesCS7D02G095500	Cytochrome P450
	TraesCS7D02G097300	Glycoside hydrolase
MQTL7D.7 (15)	TraesCS7D02G226400	Zinc finger, CCCH-type



**Table 2** continued

MQTLs (total number of CGs)	Gene ID for CG	Function description
	TraesCS7D02G227400	Protein adenylyltransferase

orthologues of rice genes could be divided into five major categories (Table 3); these are briefly described below:

- (i) *Genes involved in signaling*: Three wheat orthologues (viz., *TaSAPK6-1A*, *1B*, and *TaSAPK7-1D*) of two rice genes encoding for sucrose non-fermenting-1 related kinases (*SnRKs*) were identified in MQTL1A.5, 1B.3, and 1D.3 regions, respectively (Table 3). Overexpression of *SnRK1* increased carbon absorption and nitrogen uptake in rice (Han et al. 2016). The *SnRKs* are known to play a major role at the interface of metabolic and stress signaling, implying that they could be manipulated to boost crop performance under diverse conditions (Coello et al. 2011).
- (ii) *Genes involved in N assimilation*: Two wheat orthologues viz., *TaNiR1-6B*, *6D* of a rice nitrite reductase gene were detected in MQTL6B.2 and 6D.5 regions, respectively (Table 3). Overexpression of a ferredoxin-dependent nitrite reductase gene in *Arabidopsis* elevated NO<sub>2</sub> assimilation (Takahashi et al. 2001). In the second phase of the nitrate assimilation pathway, it catalyses the six-electron reduction of nitrite to ammonium. In addition to rice, this gene has also been cloned in various other crop plants (Han et al. 2016), including maize (Lahners et al., 1988) and *Arabidopsis* (Tanaka et al., 1994). Several genes involved in primary N uptake and assimilation have also been identified as potential bioengineering targets to increase the NUE of important crops (Li et al. 2020).
- (iii) *Genes involved in amino acid biosynthesis*: Twenty-two (22) wheat genes were identified, which are orthologous to 17 rice genes involved in the biosynthesis of different amino acids (Table 3). Of these 22 genes, two genes, *TaASN2-1A*, and *TaASN2-1B* have already been functionally characterized in wheat (reviewed in Karunarathne et al. 2020). The orthologues of these genes are key players in driving NUE in important crops and have been studied in some detail in major crops including rice and barley (Beatty et al. 2013; Han et al. 2016; Zhang et al. 2020a, 2020b). Among these genes, the GOGAT gene is found in higher plants in two antigenically distinct forms, namely, *NAD(P)H-GOGAT* and *Fd-GOGAT*. The wheat MQTL3B.3 was found to carry *TaGOGAT1-3B* and MQTL3D.3 was found to carry *TaGOGAT3D.3 gene*. These enzymes differ in size of the proteins encoded, tissue localization, and physiological roles (Esposito et al. 2005). *NAD(P)H-GOGAT* is expected to play a major role in primary N assimilation since it is regulated by N-status in the plant in response to available N (Vanoni and Curti, 1999). The deletion of the *OsNADH-GOGAT2* gene resulted in a significant reduction in yield and plant biomass in rice (Yamaya, 2011).
- (iv) *Genes encoding TFs*: Wheat MQTLs were also found to carry 9 genes (Table 3) that were orthologous to 6 rice genes encoding TFs. Among these genes, only one gene, *TaNAC9-6B* (or *GPC-B1/NAM-B1*) has been functionally characterized in wheat which is known to improve the nutrient remobilization and grain protein content (Uauy et al. 2006). The remaining genes are also important genes involved in N assimilation and their roles in N remobilization and NUE has been demonstrated in several crops (Han et al. 2016; Chiasson et al. 2014).
- (v) *Genes encoding transporters*: A total of 13 wheat orthologues of 9 rice genes encoding different transporters were also identified in different wheat MQTL regions (Table 3). These 13 wheat genes included two ammonium transporter genes (*TaAMT1.2/1.3-6B*, *6D*), 3 wheat nitrate transporter genes (viz., *TaNRT2.3-3B*, *3D*; *TaNRT2.4-7B*) of the NRT2 family (high-affinity transporters), four wheat genes (*TaNPF7.7-1A*, *1B*, *1D* and *TaNRT1-4B*) of NRT1/NPF family (low affinity transporters) and three NRT2 partner proteins (*TaNAR2.1-4A*; *TaNAR2.2-6B*, *6D*) (Table 3). In addition, a lysine histidine transporter (i.e., *TaLHT1-7A*) was detected in MQTL7A.6 region.

**Table 3** Wheat orthologues of known rice genes for NUE related functions, with names of these rice genes and effects on phenotype related with NUE

MQTL [wheat homologue]	Rice gene (encoded protein)	Effect on phenotype related with NUE
1. Genes involved in signaling		
MQTL1A.5 [ <i>TraesCS1A02G215900 (TaSAPK6-1A)</i> ]; <sup>a</sup> MQTL1B.3, 1B.4, 1B.7 [ <i>TraesCS1B02G229400 (TaSAPK6-1B)</i> ]; MQTL1D.3 [ <i>TraesCS1D02G218200 (TaSAPK6-1D)</i> ]	<i>OsSAPK6</i> (Sucrose non-fermenting-1 related kinases)	Higher NUpE
MQTL1A.5 [ <i>TraesCS1A02G215900 (TaSAPK7-1A)</i> ]	<i>OsSAPK7</i> (Sucrose non-fermenting-1 related kinases)	
2. Genes involved in N assimilation		
MQTL6B.2, 6B.3, 6B.5 [ <i>TraesCS6B02G364600 (TaNiR1-6B)</i> ]; MQTL6D.5 [ <i>TraesCS6D02G313100 (TaNiR1-6D)</i> ]	<i>OsNiR1</i> (Ferredoxin-nitrite reductase)	Increased NO <sub>2</sub> – assimilation
3. Genes involved in amino acid biosynthesis		
MQTL1A.5, 1A.6 [ <i>TraesCS1A02G085600 (TaAlaAT10-1-1A/TaAlaAT-4-1A)</i> ]; MQTL1B.3, 1B.4, 1B.7 [ <i>TraesCS1B02G102700 (TaAlaAT10-1-1B/TaAlaAT-4-1B)</i> ]	<i>OsAlaAT10-1</i> , <i>OsAlaAT4</i> (alanine aminotransferase)	Increased seed yield under low N input
MQTL5B.2 [ <i>TraesCS5B02G066600 (TaAlaAT10-2-5B)</i> ]	<i>OsAlaAT10-2</i> (alanine aminotransferase)	
MQTL1A.4, 1A.5 [ <i>TraesCS1A02G382800 (TaASN2-1A)</i> ]; MQTL1B.4, 1B.6, 1B.7 [ <i>TraesCS1B02G408200 (TaASN2-1B)</i> ]	<i>OsASN2</i> (Asparagine synthetase)	Increased seed yield and N content at high N and low N input
MQTL4B.2, MQTL4B.3, MQTL4B.4 [ <i>TraesCS4B02G194400 (TaASNI-4B)</i> ]	<i>OsASNI</i> (Asparagine synthetase)	
MQTL5B.2 [ <i>TraesCS5B02G084600 (TaAS-5B)</i> ]	<i>OsAS</i> (Asparagine synthase)	
MQTL3A.5 [ <i>TraesCS3A02G305400 (TaASP4-3A)</i> ]; MQTL3B.3 [ <i>TraesCS3B02G331100 (TaASP4-3B)</i> ]	<i>OsASP4</i> (Aspartate aminotransferase)	Increased AspAT activity
MQTL1A.5 [ <i>TraesCS1A02G160200 (TaASP6-1A)</i> ]; MQTL1B.3, 1B.4, 1B.7 [ <i>TraesCS1B02G176400 (TaASP6-1B)</i> ]; MQTL1D.3 [ <i>TraesCS1D02G157400 (TaASP6-1D)</i> ]	<i>OsASP6</i> (Aspartate aminotransferase)	
MQTL6B.3 [ <i>TraesCS6B02G393600 (TaASP1-6B)</i> ]	<i>OsASP1</i> (Aspartate aminotransferase)	
MQTL4B.2, 4B.3, 4B.4 [ <i>TraesCS4B02G240900 (TaGS1-4B)</i> ]; MQTL6B.1, 6B.2, 6B.3, 6B.4, 6B.5 [ <i>TraesCS6B02G327500 (TaGS1-6B)</i> ]	<i>OsGS1</i> (Glutamine synthetase)	Increased NUE
MQTL4B.2, 4B.3, 4B.4 [ <i>TraesCS4B02G240900 (TaGS2-4B)</i> ]	<i>OsGS2</i> (Glutamine synthetase)	
MQTL2D.5 [ <i>TraesCS2D02G251800 (TaGOX4-2D)</i> ]	<i>OsGOX4</i> (Glycolate oxidase)	
MQTL3B.3 [ <i>TraesCS3B02G299800 (TaGOGAT1/3-3B)</i> ]; MQTL3D.3 [ <i>TraesCS3D02G266400 (TaGOGAT1/3-3D)</i> ]	<i>GOGAT1</i> and <i>GOGAT3</i> (Glutamate synthase (NADPH/Ferredoxin))	Improved total N content, grain filling, and dry weight
MQTL4B.4 [ <i>TraesCS4B02G288100 (TaGGT2-4B)</i> ]	<i>OsGGT2</i> (Glutamate glyoxylate aminotransferase)	Biosynthesis and metabolism of major amino acids
MQTL4B.2, MQTL4B.3, MQTL4B.4 [ <i>TraesCS4B02G167100 (TaGGT3-4B)</i> ]	<i>OsGGT3</i> (Glutamate glyoxylate aminotransferase)	
MQTL5D.2 [ <i>TraesCS5D02G442000 (TaGDH1-5D)</i> ]	<i>OsGDH1</i> (Glutamate dehydrogenase NAD(P)H)	Increased levels of free amino acids including glutamate
4. Genes encoding transcription factors		
MQTL1A.4, 1A.5 [ <i>TraesCS1A02G411700 (TaNF-YB2.1-1A)</i> ]; MQTL1B.7 [ <i>TraesCS1B02G442000 (TaNF-YB2.1-1B)</i> ]	<i>OsNF-YB2.1</i> (Nuclear factor Y)	Increased GY
MQTL3B.3 [ <i>TraesCS3B02G385600 (TaNF-YB2.2-3B)</i> ]; MQTL3D.2, 3D.3 [ <i>TraesCS3D02G347000 (TaNF-YB2.2-3D)</i> ]	<i>OsNF-YB2.2</i> (Nuclear factor Y)	
MQTL5B.2 [ <i>TraesCS5B02G100300 (TaFBX94-5B)</i> ]	<i>OsFBX94</i> (Aberrant panicle organization)	
MQTL5B.2 [ <i>TraesCS5B02G013000 (TaHLHm4-5B)</i> ]; MQTL5D.1 [ <i>TraesCS5D02G020600 (TaHLHm4-5D)</i> ]	<i>OsHLHm4</i> (bHLH transcriptional factor)	improved N fixation and NH <sub>4</sub> + transport
MQTL4B.1 [ <i>TraesCS4B02G345800 (TaHLHm1-4B)</i> ]	<i>OsHLHm1</i> (bHLH transcriptional factor)	

**Table 3** continued

MQTL [wheat homologue]	Rice gene (encoded protein)	Effect on phenotype related with NUE
MQTL6B.4 [ <i>TraesCS6B02G075200 (TaNAC9-6B/NAM-B1)</i> ]	<i>OsNAC9/SNAC1</i> (NAM, ATAF1,2, and CUC2)	Enhanced nutrient remobilization, and grain protein content
5. Genes encoding transporters		
MQTL3B.3, 3B.6 [ <i>TraesCS3B02G285900 (TaNRT2.3-3B)</i> ]; MQTL3D.3 [ <i>TraesCS3D02G254900 (TaNRT2.3-3D)</i> ]	<i>OsNRT2.3</i> (Nitrate transporter 2)	Increased nitrate content and dry weight in shoots
MQTL7B.2 [ <i>TraesCS7B02G328700 (TaNRT2.4-7B)</i> ]	<i>OsNRT2.4</i> (Nitrate transporter 2)	
MQTL6B.1, 6B.4, 6B.5 [ <i>TraesCS6B02G238700 (TaNAR2.2-6B)</i> ]; MQTL6D.5 [ <i>TraesCS6D02G193100 (TaNAR2.2-6D)</i> ]	<i>OsNAR2.2</i> (NRT2 partner protein)	Increased nitrate content
MQTL1A.5 [ <i>TraesCS1A02G197600 (TaNPF7.7-1A)</i> ]; MQTL1B.3, 1B.4, 1B.7 [ <i>TraesCS1B02G212200 (TaNPF7.7-1B)</i> ]; MQTL1D.3 [ <i>TraesCS1D02G201100 (TaNPF7.7-1D)</i> ]	<i>OsNPF7.7/OsPTR10</i> (Nitrate transporter)	
MQTL4B.2, 4B.3, 4B.4 [ <i>TraesCS4B02G231500 (TaNRT1-4B)</i> ]	<i>OsNPF8.9/OsNRT1</i> (Nitrate transporter)	
MQTL4A.3, 4A.4, 4A.5, 4A.6 [ <i>TraesCS4A02G367300 (TaNAR2.1-4A)</i> ]; MQTL6B.1, 6B.4, 6B.5 [ <i>TraesCS6B02G254800 (TaAMT1.2/1.3-6B)</i> ]; MQTL6D.5 [ <i>TraesCS6D02G208200 (TaAMT1.2/1.3-6D)</i> ]	<i>OsNAR2.1</i> (NRT2 partner protein) <i>OsAMT1.2</i> and <i>OsAMT1.3</i> (Ammonium transporter)	increased ammonium uptake
MQTL7A.6 [ <i>TraesCS7A02G156600 (TaLHT1-7A)</i> ]	<i>OsLHT1</i> (Lysine histidine transporter)	improved plant performance under low N condition

<sup>a</sup>MQTLs had overlapping physical regions, therefore some wheat genes were detected repeatedly in different MQTL regions

In plants, N can be taken up either as ammonium or nitrate directly from the soil through roots. The ammonium transporter genes facilitate the movement of ammonium ions to intracellular compartments, where it is then converted into a variety of organic compounds, including amino acids, via the GS/GOGAT pathway (Oaks, 1994). Nitrate, on the other hand, is primarily carried into the cell by nitrate transporters and then converted to nitrite by nitrate reductase before being reduced to ammonium salts by nitrite reductase (Han et al. 2016; Zhang et al. 2020a, 2020b). Increasing the efficiency of N-related transporters is another biotechnological approach for improving N uptake (Zhang et al. 2020a, 2020b). Since N uptake by different transporters relies on proper carbon skeletons to allow for the synthesis of the various transported molecules, simply increasing the expression of these N-related transporters without proper carbon skeletons would not always result in an increase in NUE in plants (Hawkesford, 2012). This information is useful for the utilization of transporter genes for improving NUE in wheat.

Among the above 49 wheat orthologues occurring in wheat MQTLs, 44 showed significant expressions (>2 TPM) in different tissues. A summary of some wheat genes that were found to be orthologous to rice genes is presented in Fig. 8. The genes encoding transporter proteins, TFs,

and signaling molecules involved in signaling were found to exhibit expression in almost all tissues examined, although the highest expression was noticed in roots tissues. This suggests that these genes are involved in regulating both NU<sub>p</sub>E and NU<sub>t</sub>E, thus affecting uptake and utilization of N, affecting yield (Han et al. 2016). N assimilation genes exhibited high expression in leaves/shoots tissues, thus matching their role in N assimilation (Masclaux-Daubresse et al. 2010). Genes involved in amino acid biosynthesis showed expression in all the tissues including roots, leaves/shoots, spike organs, and grains suggesting their roles in multiple physiological functions in plants (Masclaux-Daubresse et al. 2010).

## Conclusions

The meta-QTL analysis provides stable and robust QTLs with relatively narrower CIs, thus improving their utility in MAB. In the present study, we identified 118 MQTLs for NUE and RSA; most of the MQTLs involved QTLs for both NUE and RSA, suggesting a relationship between these two traits. As many as 88 MQTLs including 9 robust major QTLs (described as breeders' QTLs) were also validated using the results from GWAS. Although, being a complex trait, NUE can not be easily improved using an

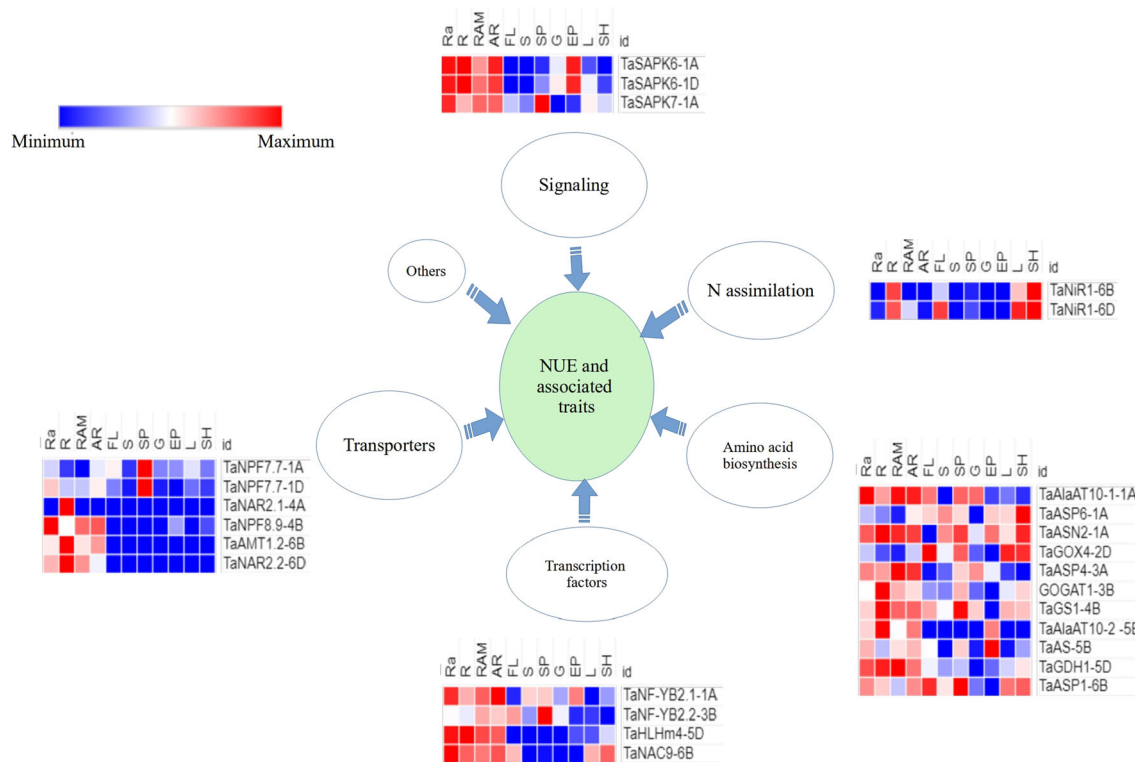


**Fig. 8** Expression patterns (shown in the form of heat maps) of some promising wheat orthologues of known genes in rice (belonging to five major categories each shown outside an arrow) in 11 different

tissues including the following: *Ra* radicle, *R* root, *RAM* root apical meristem, *AR* axillary roots, *FL* flag leaf, *S* spike, *SP* spikelets, *G* grain, *EP* embryo proper, *L* leaf, *SH* shoots

individual major MQTL, clustered MQTLs identified during the present study should prove useful for MAB. After due validation, ortho-MQTL identified in the present study can also be used across cereals.

As many as 1991 CGs underlying the 112 MQTLs were also identified during the present study; >300 of these CGs showed >5 TPM expressions in relevant plant parts/tissues. Ninety-seven (97) high confidence CGs with functions previously reported as important for studied traits were also listed for 53 robust and GWAS-verified MQTLs. These CGs may be further validated using approaches like over-expression, gene editing, and gene knockout, etc. In addition, 49 orthologues for 35 known rice NUE genes were also identified in MQTL regions, suggesting that the knowledge from rice, the model cereal, can also be utilized for the identification of useful genes in wheat. Overall, the breeder's MQTLs identified in the present study have the potential for MAB for NUE traits and the CGs are the potential targets that can be exploited using biotechnological techniques like transgenesis and gene editing for improving NUE in wheat.

**Supplementary Information** The online version contains supplementary material available at <https://doi.org/10.1007/s12298-021-01085-0>.

**Acknowledgements** The Department of Science and Technology (DST) in New Delhi, India, provided DKS with an INSPIRE fellowship, while the Head, Department of Plant Breeding and Genetics, Punjab Agricultural University in Ludhiana, India, provided the essential facilities.

**Authors contribution** PKG and PS conceived and planned the study. DKS, YC, NP and AC collected the literature and tabulated the data for meta-QTL analysis. DKS conducted the analysis. DKS and YC interpreted the results and wrote the manuscript. PKG and PS edited and finalized the manuscript with the help of DKS.

**Availability of data and material** Data generated or analysed during this study are included in this published article (and its Supplementary Material).

**Declarations**

**Conflict of interests** The authors declare that they have no competing interests.

## References

- Aduragbemi A, Soriano JM (2021) Unravelling consensus genomic regions conferring leaf rust resistance in wheat via meta-QTL analysis. bioRxiv. doi:<https://doi.org/10.1101/2021.05.11.443557>

- Ahn S, Anderson JA, Sorrells ME, Tanksley SD (1993) Homoeologous relationships of rice, wheat and maize chromosomes. *Mol Genet* 241:483–490. <https://doi.org/10.1007/BF00279889>
- Arcade A, Labourdette A, Falque M, Mangin B, Chardon F, Charcosset A, Joets J (2004) BioMercator: integrating genetic maps and QTL towards discovery of candidate genes. *Bioinformatics* 20:2324–2326. <https://doi.org/10.1093/bioinformatics/bth230>
- Balyan HS, Gahlaut V, Kumar A, Jaiswal V, Dhariwal R, Tyagi S, Agarwal P, Kumari S, Gupta PK (2016) Nitrogen and phosphorus use efficiencies in wheat: physiology, phenotyping, genetics, and breeding. *Plant Breed Rev* 40:167–234. <https://doi.org/10.1002/9781119279723.ch4>
- Beatty PH, Carroll RT, Shrawat AK, Guevara D, Good AG (2013) Physiological analysis of nitrogen-efficient rice overexpressing alanine aminotransferase under different N regimes. *Botany* 91:866–883
- Bennetzen JL, Chen M (2008) Grass genomic synteny illuminates plant genome function and evolution. *Rice* 1:109–118. <https://doi.org/10.1007/s12284-008-9015-6>
- Bi YM, Kant S, Clark J, Gidda S, Ming F, Xu J, Rochon A, Shelp BJ, Hao L, Zhao R, Mullen RT (2009) Increased nitrogen-use efficiency in transgenic rice plants over-expressing a nitrogen-responsive early nodulin gene identified from rice expression profiling. *Plant Cell Environ* 32:1749–1760
- Brasier K, Ward B, Smith J, Seago J, Oakes J, Balota M, Davis P, Fountain M, Brown-Guedira G, Sneller C, Thomason W (2020) Identification of quantitative trait loci associated with nitrogen use efficiency in winter wheat. *PLoS ONE* 15:e0228775. <https://doi.org/10.1371/journal.pone.0228775>
- Chiasson DM, Loughlin PC, Mazurkiewicz D, Mohammadidehcheshmeh M, Fedorova EE, Okamoto M, McLean E, Glass AD, Smith SE, Bisseling T, Tyerman SD (2014) Soybean SAT1 (Symbiotic Ammonium Transporter 1) encodes a bHLH transcription factor involved in nodule growth and NH<sub>4</sub><sup>+</sup> transport. *Proc Natl Acad Sci* 111:4814–4819. <https://doi.org/10.1073/pnas.1312801111>
- Cirilo AG, Dardanelli J, Balzarini M, Andrade FH, Cantarero M, Luque S, Pedrol HM (2009) Morpho-physiological traits associated with maize crop adaptations to environments differing in nitrogen availability. *Field Crops Res* 113:116–124. <https://doi.org/10.1016/j.fcr.2009.04.011>
- Cobb JN, Biswas PS, Platten JD (2019) Back to the future: revisiting MAS as a tool for modern plant breeding. *Theor Appl Genet* 132:647–667. <https://doi.org/10.1007/s00122-018-3266-4>
- Coello P, Hey SJ, Halford NG (2011) The sucrose non-fermenting-1-related (SnRK) family of protein kinases: potential for manipulation to improve stress tolerance and increase yield. *J Exp Bot* 62:883–893. <https://doi.org/10.1093/jxb/erq331>
- Collard BCY, Mackill DJ (2008) Marker-assisted selection: an approach for precision plant breeding in the twenty-first century. *Philos Trans R Soc Lond B Biol Sci* 363:557–572
- Dalton DA, Boniface C, Turner Z, Lindahl A, Kim HJ, Jelinek L, Govindarajulu M, Finger RE, Taylor CG (2009) Physiological roles of glutathione S-transferases in soybean root nodules. *Plant Physiol* 150:521–530
- Darvasi A, Soller M (1997) A simple method to calculate resolving power and confidence interval of QTL map location. *Behav Genet* 27:125–132. <https://doi.org/10.1023/a:1025685324830>
- Darzi-Ramandi H, Shariati J V, Tavakol E, Najafi-Zarini H, Bilgrami SS, Razavi K (2017) Detection of consensus genomic regions associated with root architecture of bread wheat on groups 2 and 3 chromosomes using QTL meta-analysis. *Aust J Crop Sci* 777–785.
- Do THT, Martinoia E, Lee Y, (2018) Functions of ABC transporters in plant growth and development. *Curr Opin Plant Biol* 41:32–38
- Dong NQ, Sun Y, Guo T, Shi CL, Zhang YM, Kan Y, Xiang YH, Zhang H, Yang YB, Li YC, Zhao HY (2020) UDP-glucosyltransferase regulates grain size and abiotic stress tolerance associated with metabolic flux redirection in rice. *Nat Commun* 11:1–16
- Endelman JB, Plomion C (2014) LPmerge: an R package for merging genetic maps by linear programming. *Bioinformatics* 30:1623–1624. <https://doi.org/10.1093/bioinformatics/btu091>
- Esposito S, Guerriero G, Vona V, Di Martino RV, Carfagna S, Rigano C (2005) Glutamate synthase activities and protein changes in relation to nitrogen nutrition in barley: the dependence on different plastidic glucose-6P dehydrogenase isoforms. *J Exp Bot* 56:55–64
- Fan X, Cui F, Ji J, Zhang W, Zhao X, Liu J, Meng D, Tong Y, Wang T, Li J (2019) Dissection of pleiotropic QTL regions controlling wheat spike characteristics under different nitrogen treatments using traditional and conditional QTL mapping. *Front Plant Sci* 10:187. <https://doi.org/10.3389/fpls.2019.00187>
- Forde BG (2014) Nitrogen signaling pathways shaping root system architecture: an update. *Curr Opin Plant Biol* 21:30–36
- Garnett T, Conn V, Kaiser BN (2009) Root based approaches to improving nitrogen use efficiency in plants. *Plant Cell Environ* 32:1272–1283. <https://doi.org/10.1111/j.1365-3040.2009.02011.x>
- Gaut BS (2002) Evolutionary dynamics of grass genomes. *New Phytol* 154:15–28
- Goffinet B, Gerber S (2000) Quantitative trait loci: a meta-analysis. *Genetics* 155:463–473
- Good AG, Shrawat AK, Muench DG (2004) Can less yield more? Is reducing nutrient input into the environment compatible with maintaining crop production? *Trends Plant Sci* 9:597–605. <https://doi.org/10.1016/j.tplants.2004.10.008>
- Good AG, Beatty PH (2011) Biotechnological approaches to improving nitrogen use efficiency in plants: alanine aminotransferase as a case study. In: Malcolm JH, Peter B (ed) *The molecular and physiological basis of nutrient use efficiency in crops*. Wiley, New York, pp 165–191. doi:<https://doi.org/10.1002/9780470960707>
- Greef JM (1994) Productivity of maize (*Zea mays* L.) in relation to morphological and physiological characteristics under varying amounts of nitrogen supply. *J Agron Crop Sci* 172:317–326
- Guo B, Slep DA, Lu P, Shannon JG, Nguyen HT, Arelli PR (2006) QTLs associated with resistance to soybean cyst nematode in soybean: meta-analysis of QTL locations. *Crop Sci* 46:595–602
- Guo J, Chen L, Li Y, Shi Y, Song Y, Zhang D, Li Y, Wang T, Yang D, Li C (2018) Meta-QTL analysis and identification of candidate genes related to root traits in maize. *Euphytica* 214:223. <https://doi.org/10.1007/s10681-018-2283-3>
- Han M, Wong J, Su T, Beatty PH, Good AG (2016) Identification of nitrogen use efficiency genes in barley: searching for QTLs controlling complex physiological traits. *Front Plant Sci* 7:1587
- Han G, Lu C, Guo J, Qiao Z, Sui N, Qiu N, Wang B (2020) C2H2 zinc finger proteins: master regulators of abiotic stress responses in plants. *Front Plant Sci* 11:115. <https://doi.org/10.3389/fpls.2020.00115>
- Hawkesford MJ (2012) Improving nutrient use efficiency in crops. eLS. doi:<https://doi.org/10.1002/9780470015902.a0023734>
- He X, Qu B, Li W, Zhao X, Teng W, Ma W, Ren Y, Li B, Li Z, Tong Y (2015) The nitrate-inducible NAC transcription factor *TaNAC2-5A* controls nitrate response and increases wheat yield. *Plant Physiol* 169:1991–2005
- Hirel B, Le Gouis J, Ney B, Gallais A (2007) The challenge of improving nitrogen use efficiency in crop plants: towards a more central role for genetic variability and quantitative genetics within integrated approaches. *J Exp Bot* 58:2369–2387

- Jan I, Saripalli G, Kumar K, Kumar A, Singh R, Batra R, Sharma PK, Balyan HS, Gupta PK (2021) Meta-QTL analysis for stripe rust resistance in wheat. doi:<https://doi.org/10.21203/rs.3.rs-380807/v1>
- Jun XU, Wang XY, Guo WZ (2015) The cytochrome P450 superfamily: key players in plant development and defense. *J Integr Agr* 14:1673–1686
- Karunarathne SD, Han Y, Zhang XQ, Li C (2020) Advances in understanding the molecular mechanisms and potential genetic improvement for nitrogen use efficiency in barley. *Agronomy* 10:662. <https://doi.org/10.3390/agronomy10050662>
- Khahani B, Tavakol E, Shariati V, Fornara F (2020) Genome wide screening and comparative genome analysis for Meta-QTLs, ortho-MQTLs and candidate genes controlling yield and yield-related traits in rice. *BMC Genom* 21:294. <https://doi.org/10.1186/s12864-020-6702-1>
- Khahani B, Tavakol E, Shariati V, Rossini L (2021) Meta-QTL and ortho-MQTL analyses identified genomic regions controlling rice yield, yield-related traits and root architecture under water deficit conditions. *Sci Rep* 11:6942. <https://doi.org/10.1038/s41598-021-86259-2>
- Kumar S, Mohan A, Balyan HS, Gupta PK (2009) Orthology between genomes of Brachypodium, wheat and rice. *BMC Res Notes* 2:1–9
- Kumar IS, Nadarajah K (2020) A meta-analysis of quantitative trait loci associated with multiple disease resistance in rice (*Oryza sativa* L.). *Plants* 9:1491. doi:<https://doi.org/10.3390/plants9111491>
- Kumari S, Raghuram N (2020) Protein Phosphatases in N Response and NUE in Crops. In: Pandey G (ed) Protein phosphatases and stress management in plants. Springer, Switzerland, pp 233–244
- Kumari S, Sharma N, Raghuram N (2021) Meta-analysis of yield-related and N-responsive genes reveals chromosomal hotspots, key processes and candidate genes for nitrogen-use efficiency in rice. *Front Plant Sci* 12:627955
- Lahners K, Kramer V, Back E, Privalle L, Rothstein S (1988) Molecular cloning of complementary DNA encoding maize nitrite reductase: molecular analysis and nitrate induction. *Plant Physiol* 88:741–746
- Li P, Chen F, Cai H, Liu J, Pan Q, Liu Z, Gu R, Mi G, Zhang F, Yuan L (2015) A genetic relationship between nitrogen use efficiency and seedling root traits in maize as revealed by QTL analysis. *J Exp Bot* 66:3175–3188. <https://doi.org/10.1093/jxb/erv127>
- Li X, Zeng R, Liao H (2016) Improving crop nutrient efficiency through root architecture modifications. *J Integr Plant Biol* 58:193–202
- Li M, Xu J, Gao Z, Tian H, Gao Y, Kariman K (2020) Genetically modified crops are superior in their nitrogen use efficiency: a meta-analysis of three major cereals. *Sci Rep* 10:1–9
- Liu R, Zhang H, Zhao P, Zhang Z, Liang W, Tian Z, Zheng Y (2012) Mining of candidate maize genes for nitrogen use efficiency by integrating gene expression and QTL data. *Plant Mol Biol Rep* 30:297–308. <https://doi.org/10.1007/s11105-011-0346-x>
- López-Bucio J, Cruz-Ramirez A, Herrera-Estrella L (2003) The role of nutrient availability in regulating root architecture. *Curr Opin Plant Biol* 6:280–287
- Marone D, Russo MA, Laidò G, De Vita P, Papa R, Blanco A, Gadaleta A, Rubiales D, Mastrangelo AM (2013) Genetic basis of qualitative and quantitative resistance to powdery mildew in wheat: from consensus regions to candidate genes. *BMC Genom* 14:562. <https://doi.org/10.1186/1471-2164-14-562>
- Marowa P, Ding A, Kong Y (2016) Expansins: roles in plant growth and potential applications in crop improvement. *Plant Cell Rep* 35:949–965
- Masclaux-Daubresse C, Daniel-Vedele F, Dechorgnat J, Chardon F, Gaufichon L, Suzuki A (2010) Nitrogen uptake, assimilation and remobilization in plants: challenges for sustainable and productive agriculture. *Ann Bot* 105:1141–1157
- Meijón M, Satbhai SB, Tsuchimatsu T, Busch W (2014) Genome-wide association study using cellular traits identifies a new regulator of root development in Arabidopsis. *Nat Genet* 46:77–81. <https://doi.org/10.1038/ng.2824>
- Meister R, Rajani MS, Schachtman RD, DP, (2014) Challenges of modifying root traits in crops for agriculture. *Trends Plant Sci* 19:779–788
- Minic Z (2008) Physiological roles of plant glycoside hydrolases. *Planta* 227:723–740
- Misztal I (2006) Challenges of application of marker assisted selection: a review. *Anim Sci Pap Rep* 24:5–10
- Moll RH, Kamprath EJ, Jackson WA (1982) Analysis and interpretation of factors which contribute to efficiency of nitrogen utilization. *Agron J* 74:562. <https://doi.org/10.2134/agronj1982.00021962007400030037x>
- Mosleth EF, Wan Y, Lysenko A, Chope GA, Penson SP, Shewry PR, Hawkesford MJ (2015) A novel approach to identify genes that determine grain protein deviation in cereals. *Plant Biotechnol J* 13:625–635
- Oaks A (1994) Primary nitrogen assimilation in higher plants and its regulation. *Can J Bot* 72:739–750
- de Oliveira Y, Sosnowski O, Charcosset A, Joets J (2014) BioMercator 4: a complete framework to integrate QTL, meta-QTL, and genome annotation. In: European Conference on Computational Biology 2014 Sep 2014, Strasbourg, France
- Qu B, He X, Wang J, Zhao Y, Teng W, Shao A, Zhao X, Ma W, Wang J, Li B, Li Z (2015) A wheat CCAAT box-binding transcription factor increases the grain yield of wheat with less fertilizer input. *Plant Physiol* 167:411–423
- Quraishi UM, Abrouk M, Bolot S, Pont C, Throude M, Guilhot N, Confolent C, Bortolini F, Praud S, Murigneux A, Charmet G (2009) Genomics in cereals: from genome-wide conserved orthologous set (COS) sequences to candidate genes for trait dissection. *Funct Integr Genom* 9:473–484
- Quraishi UM, Abrouk M, Murat F, Pont C, Foucrier S, Desmaizieres G, Confolent C, Riviere N, Charmet G, Paux E, Murigneux A (2011) Cross-genome map based dissection of a nitrogen use efficiency ortho-metaQTL in bread wheat unravels concerted cereal genome evolution. *Plant J* 65:745–756. <https://doi.org/10.1111/j.1365-313X.2010.04461.x>
- Ramírez-González RH, Borrill P, Lang D, Harrington SA, Brinton J, Venturini L, Davey M, Jacobs J, Van Ex F, Pasha A, Khedikar Y (2018) The transcriptional landscape of polyploid wheat. *Science*. <https://doi.org/10.1126/science.aar6089>
- Raun WR, Johnson GV (1999) Improving nitrogen use efficiency for cereal production. *Agronomy* 91:357–363
- Saini DK, Srivastava P, Pal N, Gupta PK (2021) Meta-QTLs, ortho-metaQTLs and candidate genes for grain yield and associated traits in wheat (*Triticum aestivum* L.). doi:<https://doi.org/10.21203/rs.3.rs-430452/v1>
- Salarpour M, Pakniyat H, Abdolshahi R, Heidari B, Razi H, Afzali R (2020) Mapping QTL for agronomic and root traits in the Kukri/RAC875 wheat (*Triticum aestivum* L.) population under drought stress conditions. *Euphytica* 216:1–19
- Singh K, Batra R, Sharma S, Saripalli G, Gautam T, Singh R, Pal S, Malik P, Kumar M, Jan I, Singh S (2021) WheatQTLdb: a QTL database for wheat. *Mol Genet Genom*. <https://doi.org/10.1007/s00438-021-01796-9>
- Somers DJ, Isaac P, Edwards K (2004) A high-density microsatellite consensus map for bread wheat (*Triticum aestivum* L.). *Theor Appl Genet* 109:1105–1114. <https://doi.org/10.1007/s00122-004-1740-7>

- Soriano JM, Alvaro F (2019) Discovering consensus genomic regions in wheat for root-related traits by QTL meta-analysis. *Sci Rep* 9:10537. <https://doi.org/10.1038/s41598-019-47038-2>
- Sosnowski O, Charcosset A, Joets J (2012) BioMercator V3: an upgrade of genetic map compilation and quantitative trait loci meta-analysis algorithms. *Bioinformatics* 28:2082–2083. <https://doi.org/10.1093/bioinformatics/bts313>
- Sun JJ, Guo Y, Zhang GZ, Gao MG, Zhang GH, Kong FM, Zhao Y, Li SS (2013) QTL mapping for seedling traits under different nitrogen forms in wheat. *Euphytica* 191:317–331. <https://doi.org/10.1007/s10681-012-0834-6>
- Sun Y, Hu Z, Wang X, Shen X, Hu S, Yan Y, Kant S, Xu G, Xue Y, Sun S (2021) Overexpression of *OsPHR3* improves growth traits and facilitates nitrogen use efficiency under low phosphate condition. *Plant Physiol Biochem* 166:712–722
- Takahashi M, Sasaki Y, Ida S, Morikawa H (2001) Nitrite reductase gene enrichment improves assimilation of NO<sub>2</sub> in Arabidopsis. *Plant Physiol* 126:731–741
- Tanaka S, Ida S, Irifune K, Oeda K, Morikawa H (1994) Nucleotide sequence of a gene for nitrite reductase from Arabidopsis thaliana. *DNA Seq* 5:57–61
- Tiong J, Sharma N, Sampath R, MacKenzie N, Watanabe S, Metot C, Lu Z, Skinner W, Lu Y, Kridl J, Baumann U (2021) Improving nitrogen use efficiency through overexpression of alanine aminotransferase in rice, wheat, and barley. *Front Plant Sci* 12:29
- Uauy C, Distelfeld A, Fahima T, Blechl A, Dubcovsky J (2006) A NAC gene regulating senescence improves grain protein, zinc, and iron content in wheat. *Science* 314:1298–1301
- Vanoni MA, Curti B (1999) Glutamate synthase: a complex iron-sulfur flavoprotein. *Cell Mol Life Sci* 55:617–638
- Venske E, Dos Santos RS, Farias DD, Rother V, da Maia LC, Pegoraro C, Costa de Oliveira A (2019) Meta-analysis of the QTLome of fusarium head blight resistance in bread wheat: Refining the current puzzle. *Front Plant Sci* 10:727. <https://doi.org/10.3389/fpls.2019.00727>
- Veyrieras J-B, Goffinet B, Charcosset A (2007) MetaQTL: a package of new computational methods for the meta-analysis of QTL mapping experiments. *BMC Bioinform* 8:49. <https://doi.org/10.1186/1471-2105-8-49>
- Vidal EA, Alvarez JM, Araus V, Riveras E, Brooks MD, Krouk G, Ruffel S, Lejay L, Crawford NM, Coruzzi GM, Gutiérrez RA (2020) Nitrate in 2020: thirty years from transport to signaling networks. *Plant Cell* 32:2094–2119
- Wagner GP, Kin K, Lynch VJ (2013) A model based criterion for gene expression calls using RNA-seq data. *Theory Biosci* 132:159–164. <https://doi.org/10.1007/s12064-013-0178-3>
- Xiang J, Qian K, Zhang Y, Chew J, Liang J, Zhu J, Zhang Y, Fan X (2021) *OsLSD1.1* is involved in the photosystem II reaction and affects nitrogen allocation in rice. *Plant Physiol Biochem*. <https://doi.org/10.1016/j.plaphy.2021.06.004>
- Xu J, Wang X, Guo W (2015) The cytochrome P450 superfamily: Key players in plant development and defense. *J Integr Agric* 14:1673–1686. [https://doi.org/10.1016/S2095-3119\(14\)60980-1](https://doi.org/10.1016/S2095-3119(14)60980-1)
- Yamaya T (2011) Disruption of a novel *NADH-glutamate synthase2* gene caused marked reduction in spikelet number of rice. *Front Plant Sci* 2:57
- Yang X, Xia X, Zeng Y, Nong B, Zhang Z, Wu Y, Tian Q, Zeng W, Gao J, Zhou W, Liang H (2020) Genome-wide identification of the peptide transporter family in rice and analysis of the PTR expression modulation in two near-isogenic lines with different nitrogen use efficiency. *BMC Plant Biol* 20:193. <https://doi.org/10.1186/s12870-020-02419-y>
- Yang Y, Amo A, Wei D, Chai Y, Zheng J, Qiao P, Cui C, Lu S, Chen L, Hu YG (2021) Large-scale integration of meta-QTL and genome-wide association study discovers the genomic regions and candidate genes for yield and yield-related traits in bread wheat. *Theor Appl Genet* 134:1–27
- Yu J, Xuan W, Tian Y, Fan L, Sun J, Tang W, Chen G, Wang B, Liu Y, Wu W, Liu X (2021) Enhanced *OsNLP4-OsNiR* cascade confers nitrogen use efficiency by promoting tiller number in rice. *Plant Biotechnol J* 19:167–176
- Zhang Y, Yu C, Lin J, Liu J, Liu B, Wang J, Huang A, Li H, Zhao T (2017) *OsMPH1* regulates plant height and improves grain yield in rice. *PLoS ONE* 12:e0180825. <https://doi.org/10.1371/journal.pone.0180825>
- Zhang N, Zhang X, Song L, Su Q, Zhang S, Liu J, Zhang W, Fu X, Zhao M, Sun L, Ji J (2020a) Identification and validation of the superior alleles for wheat kernel traits detected by genome-wide association study under different nitrogen environments. *Euphytica* 216:1–15
- Zhang Z, Gao S, Chu C (2020b) Improvement of nutrient use efficiency in rice: current toolbox and future perspectives. *Theor Appl Genet* 133:1365–1384
- Zhao X, Peng Y, Zhang J, Fang P, Wu B (2018) Identification of QTLs and meta-QTLs for seven agronomic traits in multiple maize populations under well-watered and water-stressed conditions. *Crop Sci* 58:507–520

**Publisher's Note** Springer Nature remains neutral with regard to jurisdictional claims in published maps and institutional affiliations.